



“Extreme Highest” and “Extreme Anomalous”: Proposed indices for chlorophyll-a extreme events in European seas between 2003 and 2021

Yolanda Sagarminaga^{*}, Ángel Borja, Almudena Fontán

AZTI, Marine Research, Basque Research and Technology Alliance (BRTA), Herrera Kaia, Portualdea z/g, 20110 Pasaia, Spain

ARTICLE INFO

Edited by Dr. Menghua Wang

Keywords:

Extreme climate events
Chlorophyll-a
Satellite data
European seas
Thresholds
Seasonality
Trends

ABSTRACT

This study addresses the occurrence of extreme values of chlorophyll-a concentrations in European seas, using the satellite's OBP MODIS AQUA v2018 dataset, for the 2003–2021 period. Two novel and complementary statistical indices based on the combination of the overall period's and the monthly 90th percentiles (P90 and mP90, respectively) are proposed: (i) the Extreme Highest exceedances (EH) include the observations with highest chlorophyll-a magnitudes in each location (larger than P90 and mP90); (ii) the Extreme Anomalous exceedances (EA) address the observations larger than mP90 but lower than P90, thus representing relevant anomalies during low phytoplankton growing seasons. Given the important differences of available observations per pixel, the EH and EA exceedances are normalized and also presented in percentage units.

Although the occurrence of these indices greatly varies in time and space, the aggregated statistics and maps reveal some clear patterns: EH and EA have very distinct (almost complementary) seasonal and spatial distribution, EH prevail in mesotrophic and euphotic waters during the main interannual bloom season whilst EA are more abundant in oligotrophic waters out of the main seasonal bloom in each area. Both significant ($p < 0.05$) increasing and decreasing annual trends have been found in different European Seas. Overall, these EH and EA trends are reflecting the climate-driven physical and ecological changes in European Seas. Although these results and the conceptual and computational simplicity of these indices are encouraging, further ground truth testing is required to account for their uncertainties, mostly related to data representativeness and the performance of the chlorophyll-a estimation algorithms.

1. Introduction

In the last years, the study of “Extreme Climate Events” (ECEs) in the ocean, has been mostly concentrated on abiotic parameters such as sea-level, marine heat waves, cold spells, and extreme waves (Bailey and Van De Pol, 2016; Ren et al., 2018; IPCC, 2022a, 2022b). Extreme events of biogeochemical properties, such as chlorophyll-a concentration, have received less attention despite their high impact on marine ecosystem functioning and services, and their cascading effects (Gutschick and BassiriRad, 2003; Ummenhofer and Meehl, 2017; Van de Pol et al., 2017; Di Biagio et al., 2020; United Nations, 2021).

The occurrence of extreme chlorophyll-a values is related to intense phytoplankton blooms that may entail adverse events such as eutrophication and toxic events produced by Harmful Algae Blooms (HABs) (IPCC, 2022a). Globally, these events represent an important concern in many coastal and marine areas (IPCC, 2022b). In Europe, eutrophication problems affect about 563,000 km² (or 23%) of the marine areas

assessed by the European Environment Agency (Environmental European Agency, 2019). HABs incidence is also increasing in different European marine regions (Vasconcelos, 2013; Glibert et al., 2018; Zingone et al., 2020). HABs are responsible for important adverse socio-economic impacts related to aquaculture, health hazards for human consumption of fish and shellfish, tourism and recreational activities, and human well-being (Berdalet et al., 2015; Sanseverino et al., 2016).

The occurrence of extreme values of chlorophyll-a does not always lead to toxic or eutrophication events (Cloern, 2001; Wei et al., 2008), as other physical or biological conditions need to concur (i.e., oxygen availability, presence of toxic phytoplankton species, etc.). Nevertheless, both types of events are generally associated with steep increases of phytoplankton cells. Therefore, the identification of locations and periods of extreme chlorophyll-a values may help to point out to the most hazardous zones and dates for their occurrence and their tendencies. This information can be useful to define and implement adequate monitoring and management measures under policies such as the

^{*} Corresponding author.

E-mail addresses: ysagarminaga@azti.es (Y. Sagarminaga), aborja@azti.es (Á. Borja), afontan@azti.es (A. Fontán).

<https://doi.org/10.1016/j.rse.2023.113885>

Received 18 April 2023; Received in revised form 23 October 2023; Accepted 25 October 2023

0034-4257/© 2023 The Authors. Published by Elsevier Inc. This is an open access article under the CC BY license (<http://creativecommons.org/licenses/by/4.0/>).

European Water Framework Directive (WFD) 2000/60/EC or the Marine Strategy Framework Directive (MSFD) 2008/56/EC (Borja et al., 2010).

Different types of metrics can be used for ‘extreme indices’ (Smith, 2011). These can be based on the probability of occurrence of given quantities, on quantitative thresholds, or related to the length or persistence of the events. Indices based on the occurrence probability may include the number, percentage, or fraction of days with observation values below the 1th, 5th, or 10th percentiles, or above the 90th, 95th, or 99th percentile values. They are generally defined for given time frames (days, month, season, annual) with respect to a reference time period (i.e. 1981–2010) (IPCC, 2012). These extreme indices reflect rather ‘moderate extremes’, as more uttermost ‘extremes’ are usually investigated using Extreme Value Theory (EVT). (Kinnison, 1983; Coles, 2001), which is based in the estimation of the probability of very distant values in a distribution (generally <1 to 5% of the considered overall sample).

Concerning the indices based on quantitative thresholds, to our knowledge, there are no universally accepted thresholds or scales to define extreme values of chlorophyll-a in marine waters. In fact, due to the high heterogeneity of chlorophyll-a dynamics across marine ecosystems (Winder and Cloern, 2010), the definition of absolute values’ scales or thresholds of chlorophyll-a is hardly applicable for large scale studies. Most of the classifications, scales or thresholds proposed in the literature for marine chlorophyll-a are linked to local studies focusing on eutrophication or HABs events (Ferreira et al., 2011; Sutula et al., 2017), or as thresholds for setting legal limits for healthy seafood, drinking waters or bathing quality (World Health Organisation, 2003). Most often, these thresholds are also adapted to local or regional scopes.

In previous studies on extreme indices of chlorophyll-a in marine systems, Gohin et al. (2008) used the 90th percentile of satellite chlorophyll-a during the productive period (March to October) to identify eutrophication risk in coastal waters along the French Atlantic coast and the English Channel. Novoa et al. (2012) also used the 90th percentile for satellite data in the southeastern coast of the Bay of Biscay, and the 2005–2010 period to classify water quality status under the WFD. Borja et al. (2019) used the 90th percentile of chlorophyll-a between 2009 and 2014 to assess the quality status for Descriptor 5 (eutrophication) of the MSFD in a pan-European marine environmental status assessment. Di Biagio (2016) and Di Biagio et al. (2020) used the occurrences of 99th percentile to analyze chlorophyll-a extremes in the Mediterranean Sea, based on data from a coupled hydrodynamic-biogeochemical model. In addition, the WFD intercalibration exercise, sets the 90th percentile as a reference for the chlorophyll-a indicator in different European countries’ marine waters (European Commission, 2018).

In this context, this study aims: (i) to propose an approach to define and identify chlorophyll-a extreme indices and events (metrics and method) applicable at large scales, in this case covering all the European seas, and (ii) to calculate the spatial and temporal occurrence and trends of these events across the different primary production regimes found in the European regional seas.

2. Data and methods

The MODIS-AQUA v2018 (NASA-Ocean Biology Processing Group, 2018) reprocessed dataset was used in this study. The files downloaded from <https://oceandata.sci.gsfc.nasa.gov/directdataaccess/Level-3%20Mapped/Aqua-MODIS>, correspond to the daily, 4 km, “Chlorophyll Concentration, OCI Algorithm” product (Hu et al., 2012) expressed in mg m^{-3} . The OCI algorithm applied in the dataset, is an empirical model combining a three-band difference color index (CI) for low chlorophyll-a concentrations ($<0.15 \text{ mg m}^{-3}$), and the formerly used OCx band ratio algorithms (O’Reilly et al., 2000) for higher chlorophyll-a values. The MODIS-AQUA v2018 reprocessed dataset implements instrument calibration and vicarious calibration updates but the algorithms are identical to those employed in the R2014.0 multi-mission reprocessed

dataset. According to the dataset documentation, MODIS-AQUA v2018 significantly improve the agreement between MODIS AQUA-retrieved and in situ chlorophyll from SeaBASS data, with a notable reduction in mean bias from 32% to 18%. (<https://seabass.gsfc.nasa.gov/search/#val>, <https://oceancolor.gsfc.nasa.gov/data/reprocessing/r2018/aqua/>, Franz et al., 2018). However, the performance of this algorithm in complex optical waters (case-2 waters) like those found near coasts or in enclosed seas like the Baltic Sea or the Black Sea, are still low (Suslin and Churilova, 2016; Pitarch et al., 2016; Hu et al., 2019; Brando et al., 2021; Lavigne et al., 2021; Tilstone et al., 2021). The retrieval of accurate chlorophyll-a concentrations in coastal waters using remote sensing data remains an important challenge despite the development of several improved algorithms and procedures worldwide (Suslin and Churilova, 2016; Hu et al., 2019; O’Reilly and Werdell, 2019; Brando et al., 2021; Lavigne et al., 2021; Sathyendranath et al., 2021; European Union-Copernicus Marine Service, 2022).

This dataset was finally selected because of (i) its extended spatial coverage (covering all European regional seas), (ii) its wide temporal range (2003–2021), (iii) its homogeneity in terms of data origin (single sensor and platform) and processing methodology that restricts the causes of data uncertainties and eludes issues related to multi-sensor data merging and cross-calibration procedures (Morozov et al., 2010; Maritorena et al., 2010; Sathyendranath et al., 2017; Staehr et al., 2022; Gómez-Jakobsen et al., 2022), and (iv) its adequate spatio-temporal resolution for European seas scale (4 km pixel size and daily satellite passes). It is important to bear in mind that despite the daily passes of satellite, the dataset has observation gaps, usually due to cloud and ice coverage, that prevent having satellite ocean color observations under those conditions.

The downloaded data files were geographically subsetted to a geographical extent from 24°N to 90°N and from 45°W to 69°E, to cover the whole European regional seas. Then, they were processed to add a time dimension and merged to a 3D data cube from which the successive indices and statistics were computed. A schema of the series of analyses done and their main outcomes is presented in Fig. 1.

Initially, the 90th percentile of the chlorophyll-a values for the whole 2003–2021 period (hereafter P90) was calculated for each pixel as a threshold to identify extreme values. This election was supported by various reasons: (i) 90th percentile is a widely used indicator for setting quality thresholds of chlorophyll-a in European marine assessments (European Commission, 2018) under the WFD and subsidiarily for the MSFD, (ii) the simplicity of its calculation, and (iii) it is a threshold independent of chlorophyll-a magnitudes and, therefore, applicable across different primary production regimes: in oligotrophic waters the P90 will be lower than in eutrophic waters but the number of exceedances will have a similar meaning.

Then, the chlorophyll-a values above the P90 were identified and counted (Exc_P90) to obtain the number of exceedances per year and per month in each pixel.

This initial analysis disclosed two important outcomes. The first one concerns the large difference in the number of available observations in different European areas and months (see Supplementary Material SM1). Large gaps of data are found in high latitudes during winter months. The Mediterranean accounts for the largest number of daily observations, varying from 10% in winter months to >50% in July and August. To consider these differences, maps of exceedances divided by the number of available observations per pixel were also produced and represented as percentages of exceedances (Fig. 1). The second important outcome is related to the seasonal patterns of P90 revealed in the monthly maps of P90 exceedances seemingly linked to the regional primary production cycles. A consequence of this distribution is that the highest chlorophyll-a values in months with low primary production are often lower than the overall P90 values and are not counted among the extreme exceedances. Nevertheless, these events could be locally relevant. Thus, to avoid the under-reporting of these events, the 2003–2021 climatological monthly 90th percentiles of chlorophyll-a were computed

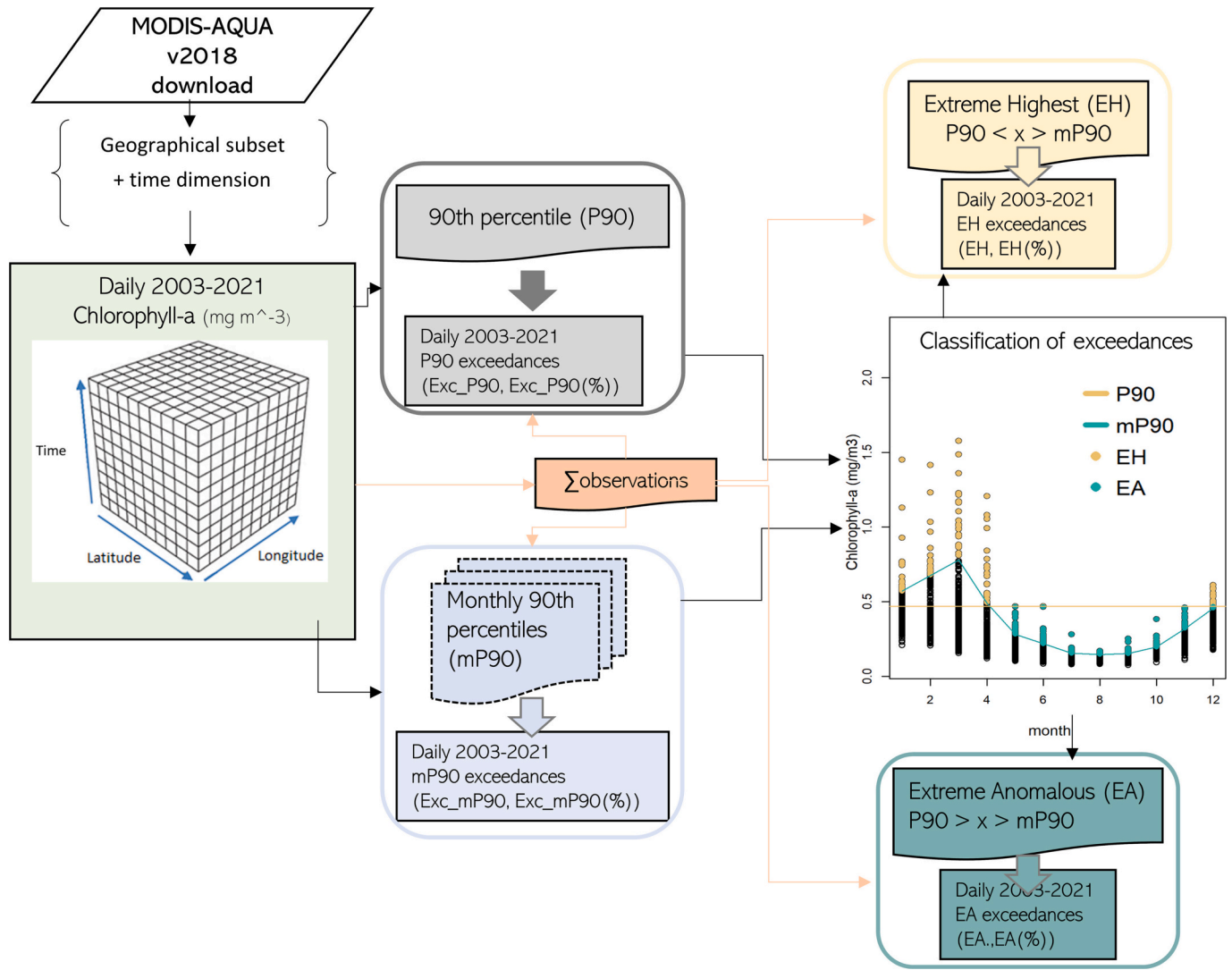


Fig. 1. Schematic representation of the analysis and outputs produced within this study. P90: 90th percentile; mP90: monthly 90th percentile; Exc_P90: Exceedances over the 90th percentile; Exc_mP90: Exceedances over the monthly 90th percentile; EH: “Extreme Highest” events and “Extreme Anomalous” events (EA).

(hereafter mP90) and the exceedances related to the mP90 were calculated in a second exceedances series (Exc_mP90). New monthly and annual maps were generated for this data series.

The comparisons of Exc_P90 and Exc_mP90, showed clear distinct monthly patterns in many areas, but the similarity of the Exc_P90 and Exc_mP90 annual maps outlined that several exceedances are counted in both series and blur the comparative conclusions of annual patterns.

To solve this, a classification of the exceedances in two groups was made (see Fig. 1): (i) chlorophyll-a values exceeding both P90 and mP90, which represent the highest chlorophyll-a values reported within each location, and (ii) the exceedances above mP90 but below P90, which include observations where chlorophyll-a magnitudes do not reach the highest 10% values in each location, but represent relevant high anomalies from the expected monthly values of chlorophyll-a (see graph in Fig. 1). Hereafter, we name the first ones as EH (Extreme Highest), and the second ones as EA (Extreme Anomalous) exceedances. The values above P90 but below mP90 are no longer considered as exceedances. This classification produces two not-overlapping series of observations, which means that an observation classified in one group is not counted in the second one. This classification also implies a conceptual distinction of extreme events, distinguishing extreme observations related to the magnitudes of chlorophyll-a (EH), and extremes related to the expected seasonal chlorophyll-a levels (EA).

Monthly and annual exceedances maps for EH and EA series were produced, both as number and as percentages of available observations.

Finally, the annual trends of exceedances for all series were calculated using the Mann-Kendall trend test (Kendall, 1975). One benefit of this test is that the data does not need to conform to any particular distribution. The test compares the relative magnitudes of sample data rather than the data values themselves (Gilbert, 1987). The Mann-Kendall Score index (S) and its associated probability (p-value) were computed to identify areas with statistically significant trends at 95% confidence level. The Sen’s slope (Sen, 1968) was calculated as an estimate of the trend magnitude. The percentages of pixels occupied by the statistically significant trends in each European regional sea (i.e. Baltic Sea, North-East Atlantic Ocean, Mediterranean Sea, and Black Sea) was calculated intersecting the trend maps with the polygons of the regional seas around Europe map (Environmental European Agency, 2022). The polygon corresponding to the outer Atlantic area that is not included in this map, was created as the difference between the total Atlantic region extent and the Atlantic subregional seas polygons.

All the former processing steps, calculations and map plots were done using the “Climate Data operators” library (Schulzweida, 2021), the R core library (R Core Team, 2020) and RStudio software (RStudio Team, 2019), including the following R packages: “ncdf4” (Pierce, 2021), “raster” (Hijmans and Van Etten, 2012), “rgdal” (Bivand et al.,

2015), “maptools” (Lewin-Koh and Bivand, 2011), “maps” (Deckmyn, 2021), “mapdata” (Deckmyn, 2018), “rasterVis” (Perpiñán and Hijmans, 2022), lattice (Sarkar, 2008), latticeExtra (Sarkar and Andrews, 2019) and trend (Pohlert, 2020). The spatial geoprocessing was done using QGIS 3.20.1-Odense (QGIS.org, 2022),

All the files created are publicly available in Zenodo’s repository (Sagarminaga, 2023).

3. Results

3.1. 90th percentile of chlorophyll-a (P90)

The P90 values of chlorophyll-a for the 2003–2021 period (Fig. 2) show big dissimilarities across the different European marine regions. These differences are associated with the heterogeneity of primary production regimes: very low P90 values ($<0.5 \text{ mg m}^{-3}$) are found in the Mediterranean Sea and the Macaronesia region; highest values ($>10 \text{ mg m}^{-3}$) are found in the Baltic Sea, in the Azov Sea and, as well as in the coastal areas of the Arctic Sea, North Sea, Celtic Seas, Iberian region and northern Black Sea. Intermediate P90 values are registered in mid and low latitudes of the Atlantic Ocean and Arctic Sea, in the Black Sea, and the coastal zones of the western Mediterranean Sea and western Adriatic Sea.

As by definition of the P90, the total number of exceedances related to P90 in each pixel corresponds to the 10% of the available observations, and thus cannot be used to assess the spatial patterns of these extreme values’ occurrences.

The monthly distribution of Exc_P90s (Fig. 3) evidences seasonality patterns: the highest Exc_P90 values occur in months coincident with the phytoplankton growing season(s) in each marine region (i.e., winter and early spring months in the Mediterranean, spring in mid latitudes and late spring and summer months in northern latitudes).

The annual distribution of Exc_P90 values (Fig. 4) shows a very high spatial and interannual variability where high exceedances spots are found in different areas each year.

3.2. Monthly 90th percentile (mP90)

The maps representing the 90th percentile of chlorophyll-a in each climatological month (mP90) (SM2), clearly confirm the seasonality patterns previously identified in the monthly Exc_P90 maps. These different mP90 seasonality cycles are better apprehended in Fig. 5, where mP90 and P90 values in 16 selected locations around European seas have been extracted and plotted. These locations were selected arbitrarily in different European seas as example purposes, info from other locations can be extracted from the published exceedances series

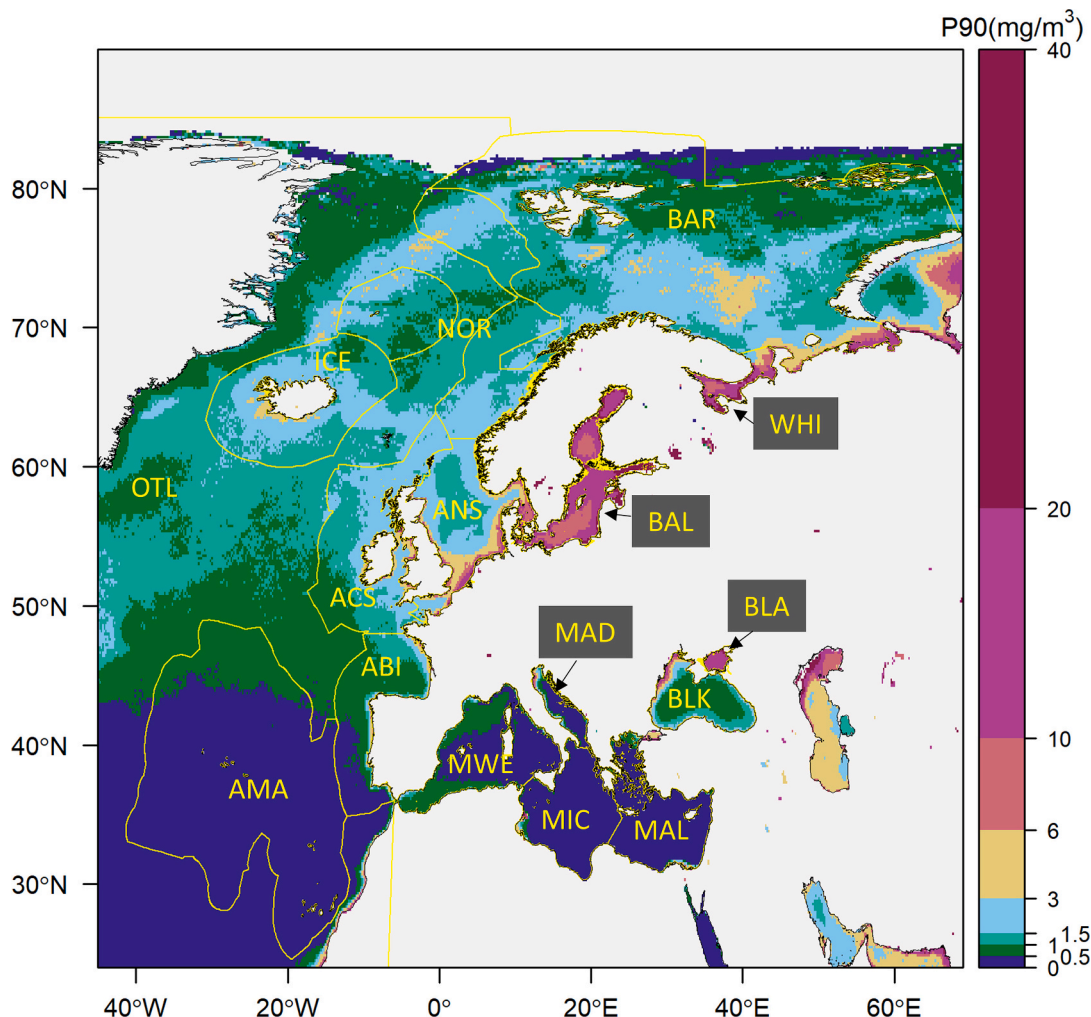


Fig. 2. Distribution of the 90th percentile (P90) of the chlorophyll-a values between 2003 and 2021 in all European seas’ subregions. The spatial extents of the regional are derived from the Regional seas around Europe map (Environmental European Agency, 2022): ABI: Bay of Biscay and the Iberian Coast; ACS: Celtic Seas; AMA: Macaronesia; ANS: Greater North Sea, incl. The Kattegat and the English Channel; BAL: Baltic Sea; BAR: Barents Sea; BLA: Black Sea - sea of Azov; BLK: Black Sea; ICE: Iceland Sea; MAD: Adriatic Sea; MAL: Aegean-Levantine Sea; MIC: Ionian Sea and the Central Mediterranean Sea; MWE: Western Mediterranean Sea; NOR: Norwegian Sea; OTL: Outer Atlantic ocean; WHI: White Sea.

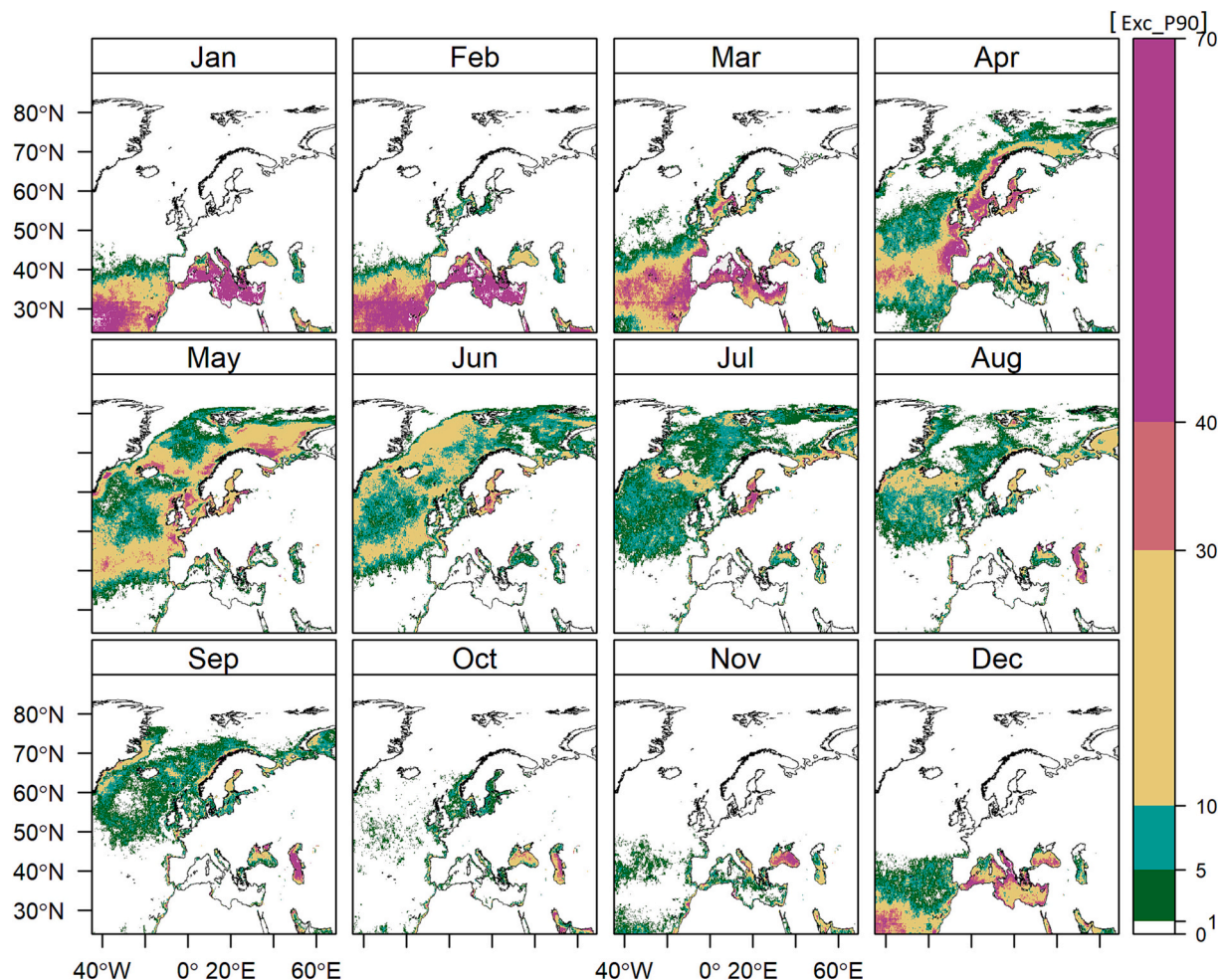


Fig. 3. Monthly distribution of Exc_P90 (chlorophyll-a exceedances related to 90th percentile during the 2003–2021 period).

(Sagarminaga, 2023).

These plots evidence the major spatial and temporal differences of mP90 values across European marine regions as well as the differences of the magnitude ranges of mP90. For instance, mP90 in the Mediterranean Sea is always below 1 mg m^{-3} , and shows a seasonal cycle with minima values in summer and maxima values in late winter or early spring. The highest values of mP90 ($>10 \text{ mg m}^{-3}$) are found in the Baltic Sea, with a primary mode in March, and a secondary peak in July–August. In the Atlantic Ocean, most locations show a seasonal pattern with a single peak in March in lower latitudes and in April–May in higher latitudes. This peak has low values in the Macaronesia region (0.30 mg m^{-3}) and high values in the English Channel (20 mg m^{-3}). Within the Black Sea region there are two distinct mP90 seasonal regimes; in the Central area the mP90 values range between 0.6 and 1.4 mg m^{-3} and show a peak in December, whereas in the northern Black Sea, the ranges are higher and wider (1.7 to 3.5 mg m^{-3}) and the seasonal pattern shows a minimum in March and a maximum in May.

The monthly exceedances related to mP90 (Exc_mP90), as per the definition of the metric, represent 10% of the available observations in each month, and thus reflect more the differences of the sample size per month, than the differences related to the extreme values occurrences.

As the maps of the yearly exceedances related to mP90 (Exc_mP90s) do not allow to identify the exceedances occurring off the growing seasons that we wanted to reveal using the mP90 thresholds, we took a step forward to use the EH and EA metrics.

3.3. Extreme highest (EH) and Extreme anomalous (EA) exceedances

Hence, as mentioned in the methods section, the exceedances were classified in two non-overlapping groups: (i) those exceeding both P90 and mP90 thresholds (EH) and (ii) the exceedances that are above mP90 but below P90 (EA).

The total number of exceedances and corresponding percentages of EH and EA sets for the whole 2003–2021 period are mapped in Fig. 6. These maps show the high difference of spatial distribution between EH and EA. They also put in evidence that some areas with low number of exceedances are in fact areas with high percentages of exceedances, outlining the importance of considering the effect of the variability of the number of observations in each pixel.

The highest EH percentages appear mostly in northern latitudes and the highest EA percentages appear in southern latitudes. Hence, 45°N seems to be a latitudinal inflexion boundary. Exceptions to this general pattern are found in the coastal and shelf areas below 45°N , in the Black Sea, the Caspian Sea, the central North Sea, and some areas of the Arctic Sea.

The monthly distributions of EH and EA percentages (Fig. 7), show that EH exceedances are found in latitudinal ranges where the seasonal growing season is taking place, winter in the latitudes below 40°N , and towards higher latitudes from spring to summer months.

The monthly EA exceedances appear mainly from January to April in the Atlantic Ocean, from April to November, in the southern and coastal European seas excepting the Baltic Sea, and in Arctic waters during July and August.

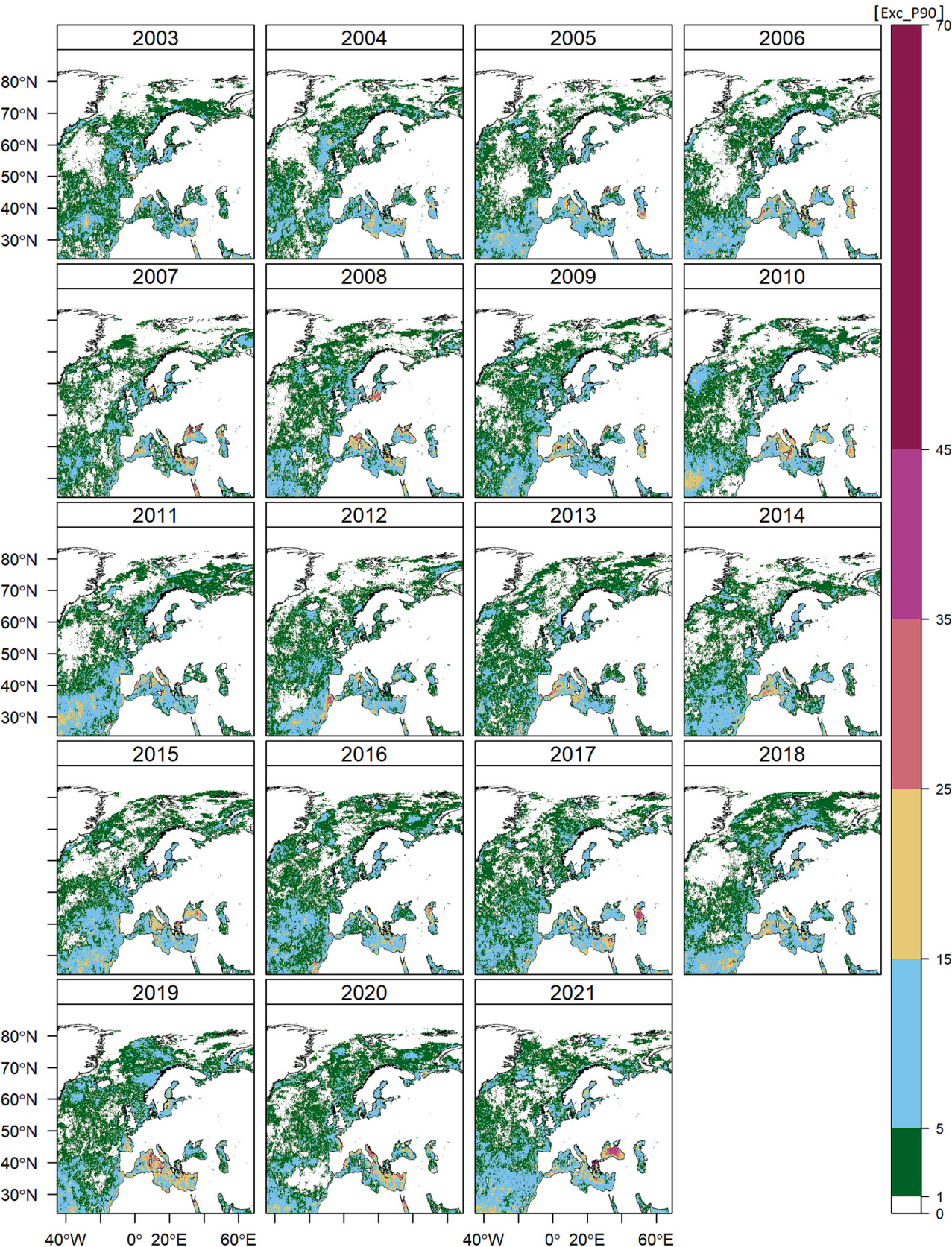


Fig. 4. Annual distribution of Exc_P90 (chlorophyll-a exceedances related to 90th percentile during the 2003–2021 period).

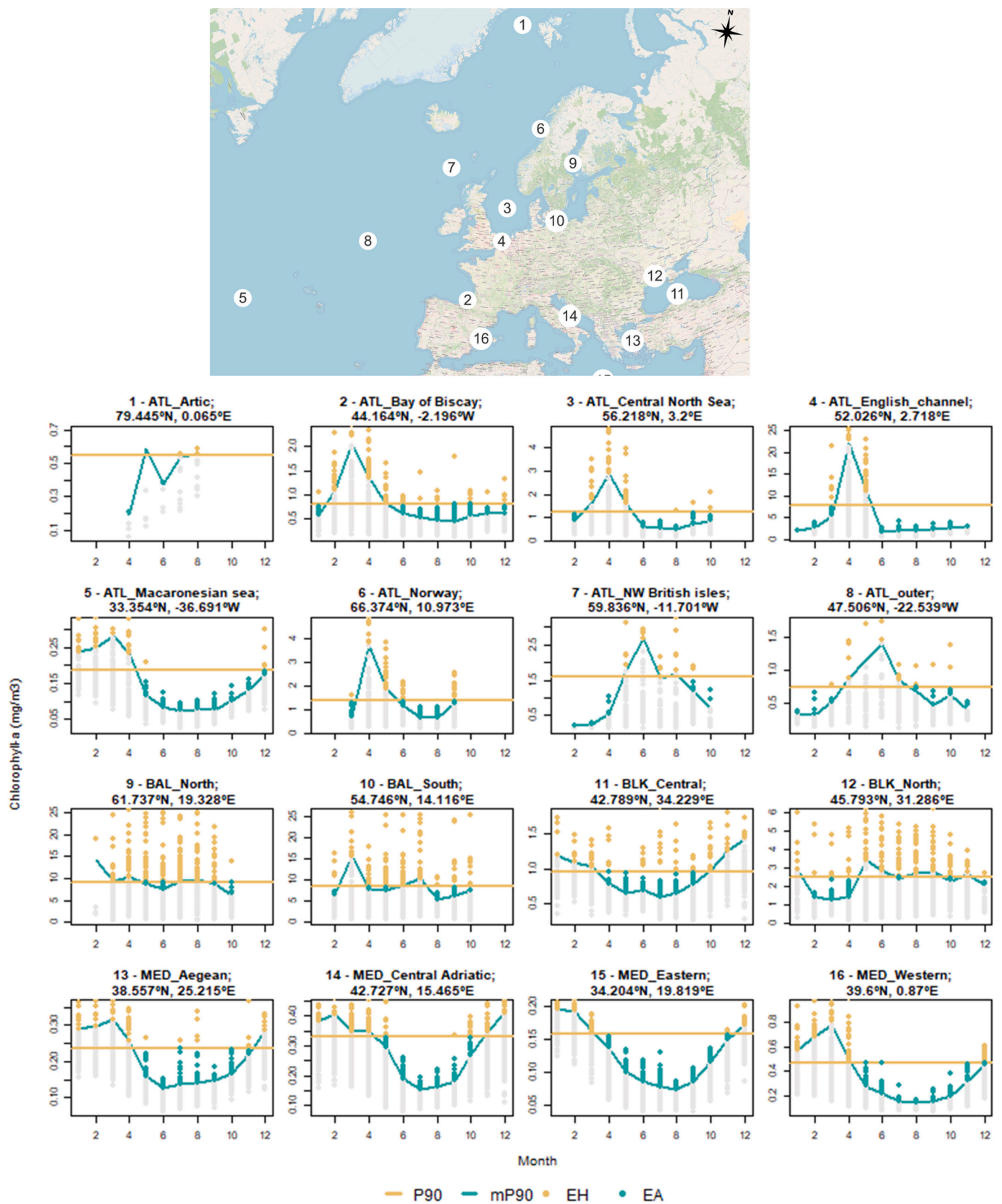


Fig. 5. Plots for 2003–2021 period's 90th percentile (P90), monthly 90th percentiles of chlorophyll-a (mP90), EH, EA and chlorophyll observations in different locations of European sea regions. ATL: Atlantic Ocean; BAL: Baltic Sea; BLK: Black Sea; MED: Mediterranean Sea.

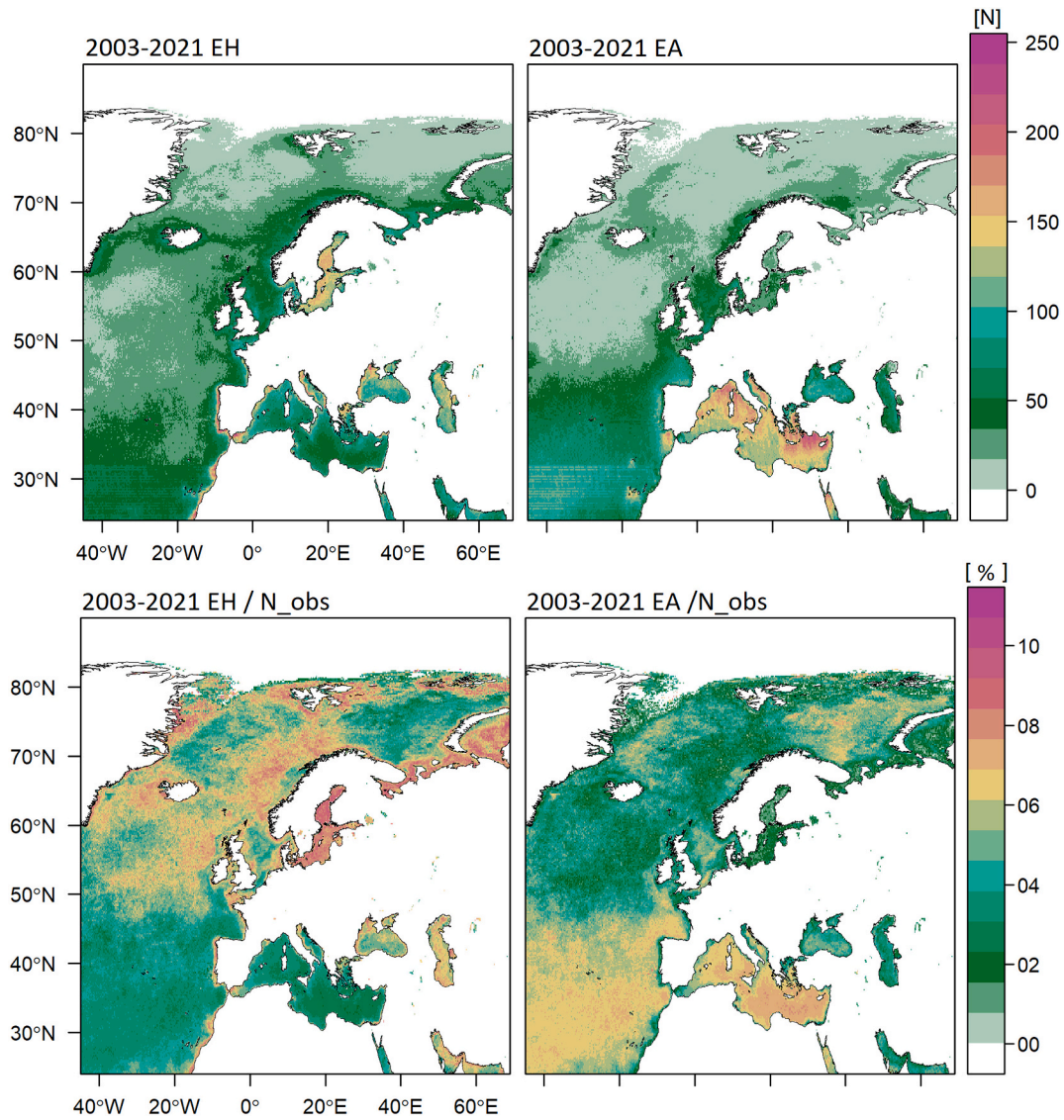


Fig. 6. Top: Total number of exceedances of extreme highest (EH) and extreme anomalous (EA) observations. Bottom: ratio between EH and EA exceedances and the available number of observations in each pixel expressed as percentage values.

The annual distribution of EH and EA percentages show a very high interannual variability in both cases (SM3 and SM4), but the annual distributions of EH and EA are different. There are areas with clear prevalence of one exceedance class (either EH or EA), and there are also some areas where high percentages of both types of exceedances occur in the same year.

Despite the large scale and temporal patterns described above it is important to keep in mind that the occurrence of these extreme chlorophyll events have a remarkably high episodic-like variability. This variability is more evident in the heatmap plots of %EH and %EA in the 16 sample locations evaluated (SM5).

3.4. Annual trends

The high interannual variability found in annual maps makes it difficult to find recurrent patterns. Thus, annual trends have been calculated with the Mann Kendall test, to identify areas in which the temporal evolution of exceedances shows some sustained evolution (Fig. 8).

The red coloured areas represent significant (p -value<0.05) increasing trends, and the blue coloured ones significant (p -value<0.05) decreasing trends.

decreasing trends.

These maps reflect that in the Atlantic Ocean, there is a combination of latitudinal ranges with significant increasing and decreasing trends concerning both EH and EA events: increasing trends appear in latitudes below 30°N, between 40°N and 50°N and above 70°N, and significant decreasing trends appear between 30°N and 40°N and in the area between the British Isles and Iceland.

The percentages of pixels occupied with EH and EA significant increasing and decreasing trends in each European subregion have been calculated using the Fig. 9 data.

Fig. 9 confirms that areas of significant increasing trends for both EH and EA prevail in most subregions except for the Black Sea, the Sea of Azov, and the Celtic Seas. Areas with EH significant increasing trends are generally bigger than those occupied by EA increasing trends in all subregions except the Iceland sea, the North Sea, the Celtic Sea, and the Bay of Biscay subregions.

Almost no areas with EA significant decreasing trends are registered in the most northern subregions (Barents Sea, White Sea, Norwegian Sea, and Baltic Sea), and in the Adriatic subregion.

The EA significant decreasing trend areas prevail over the EH decreasing areas in all the Mediterranean subregions, especially in the

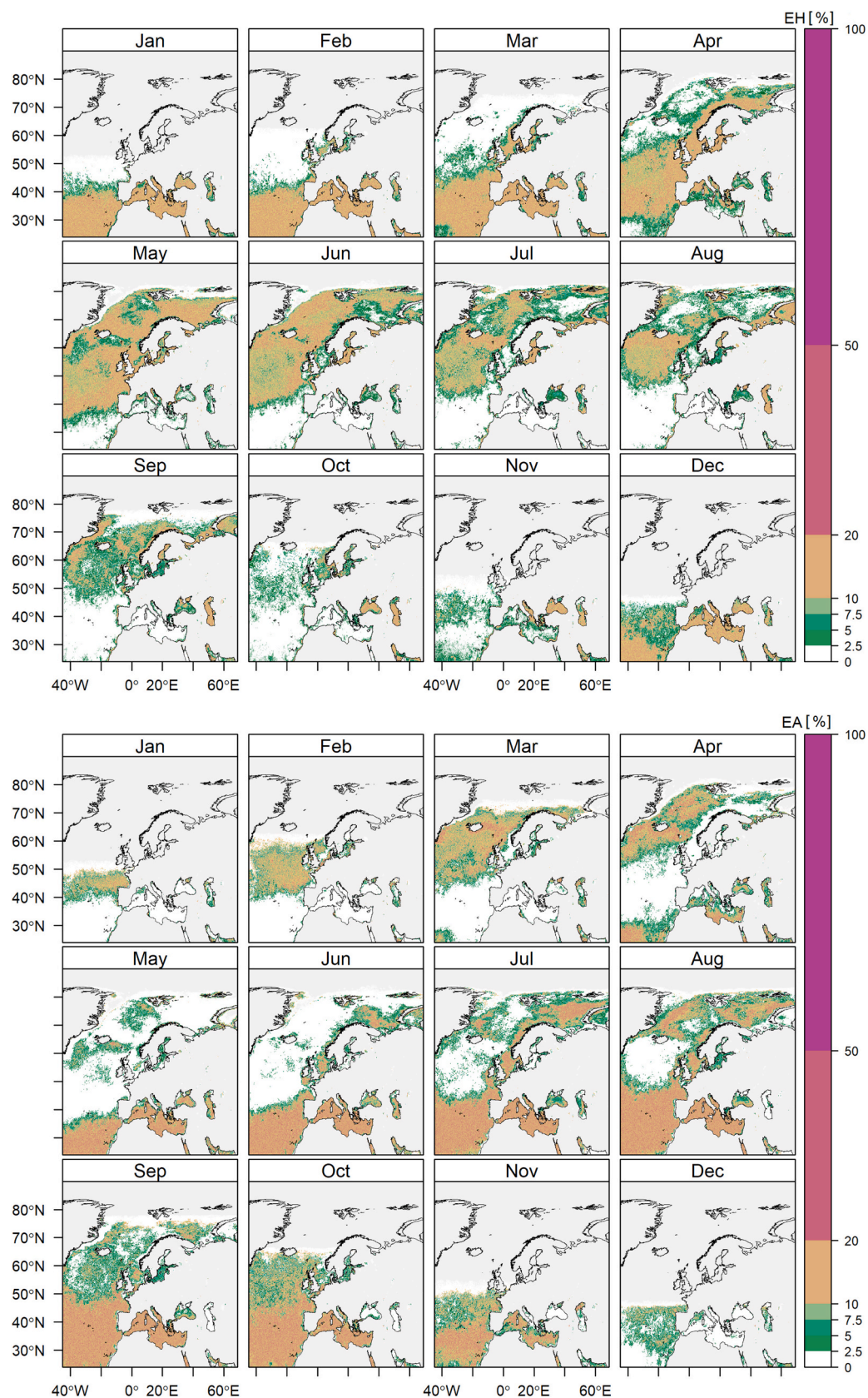


Fig. 7. Monthly distribution of extreme highest (EH) and extreme anomalous (EA) occurrences during the 2003–2021 period expressed as percentages over the number of observations.

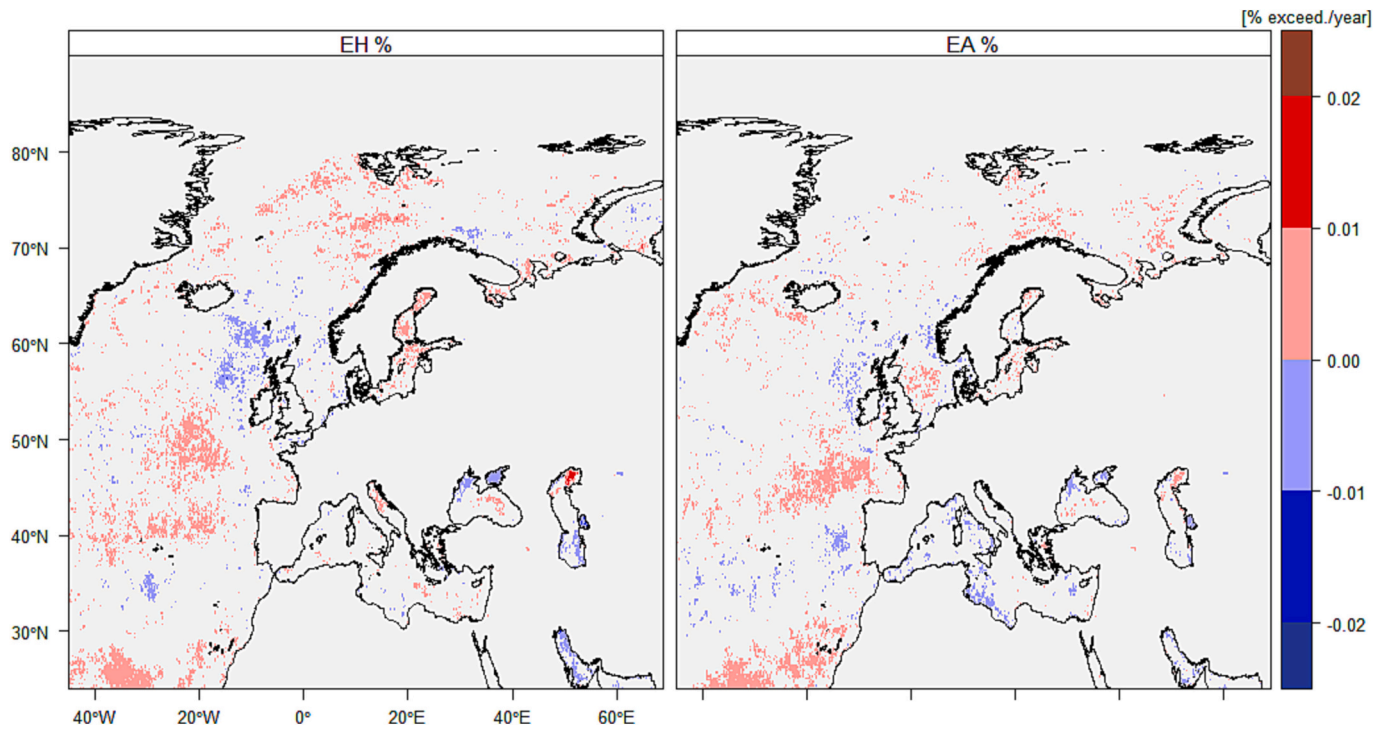


Fig. 8. Annual trend of extreme highest (EH) and extreme anomalous (EA) occurrences during the 2003–2021 period expressed as percentages over the number of observations. The legend values correspond to the Sen's slope on pixels with statistically significant Mann Kendall's score index value (p -value < 0.05). Pixels with not significant Mann Kendall's score index are represented with grey color.

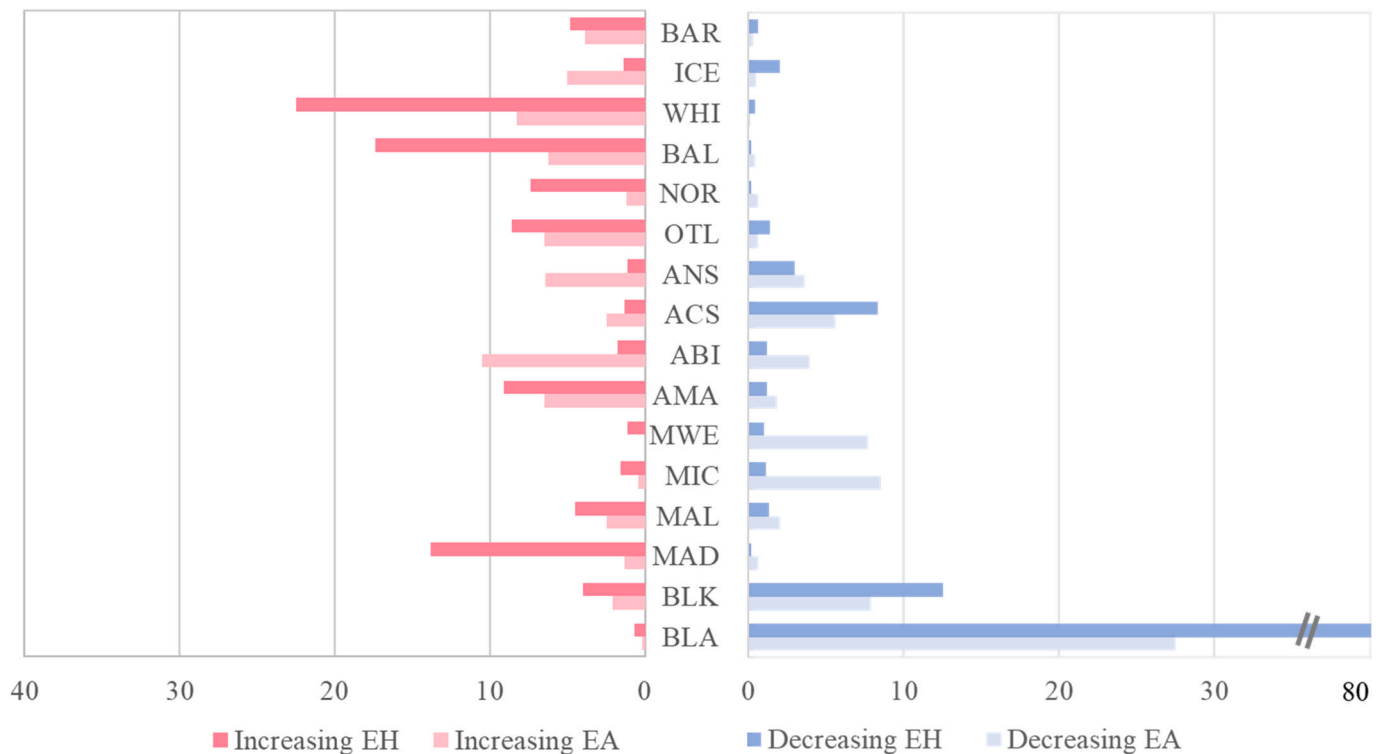


Fig. 9. Percentages of pixels occupied by significant trends (p -value < 0.05) of EH and EA between 2003 and 2021 in all European seas' subregions. ABI: Bay of Biscay and the Iberian Coast; ACS: Celtic Seas; AMA: Macaronesia; ANS: Greater North Sea, incl. The Kattegat and the English Channel; BAL: Baltic Sea; BAR: Barents Sea; BLA: Black Sea - sea of Azov; BLK: Black Sea; ICE: Iceland Sea; MAD: Adriatic Sea; MAL: Aegean-Levantine Sea; MIC: Ionian Sea and the Central Mediterranean Sea; MWE: Western Mediterranean Sea; NOR: Norwegian Sea; OTL: Outer Atlantic Ocean; WHI: White Sea.

central and western subregions.

4. Discussion

The high heterogeneity of ranges and dynamics of chlorophyll-a production across European Seas (Longhurst, 2007; Reygondeau et al.,

2013), also detected in the mP90 values calculated in this study, encourages the use of thresholds based on relative frequency metrics such as the 90th percentile for large scale studies. This approach prevents the need of defining a myriad of quantitative thresholds adapted to different areas and seasons that hamper comparative interpretation (European Commission, 2018; Macias Moy et al., 2020), as happens also in primary

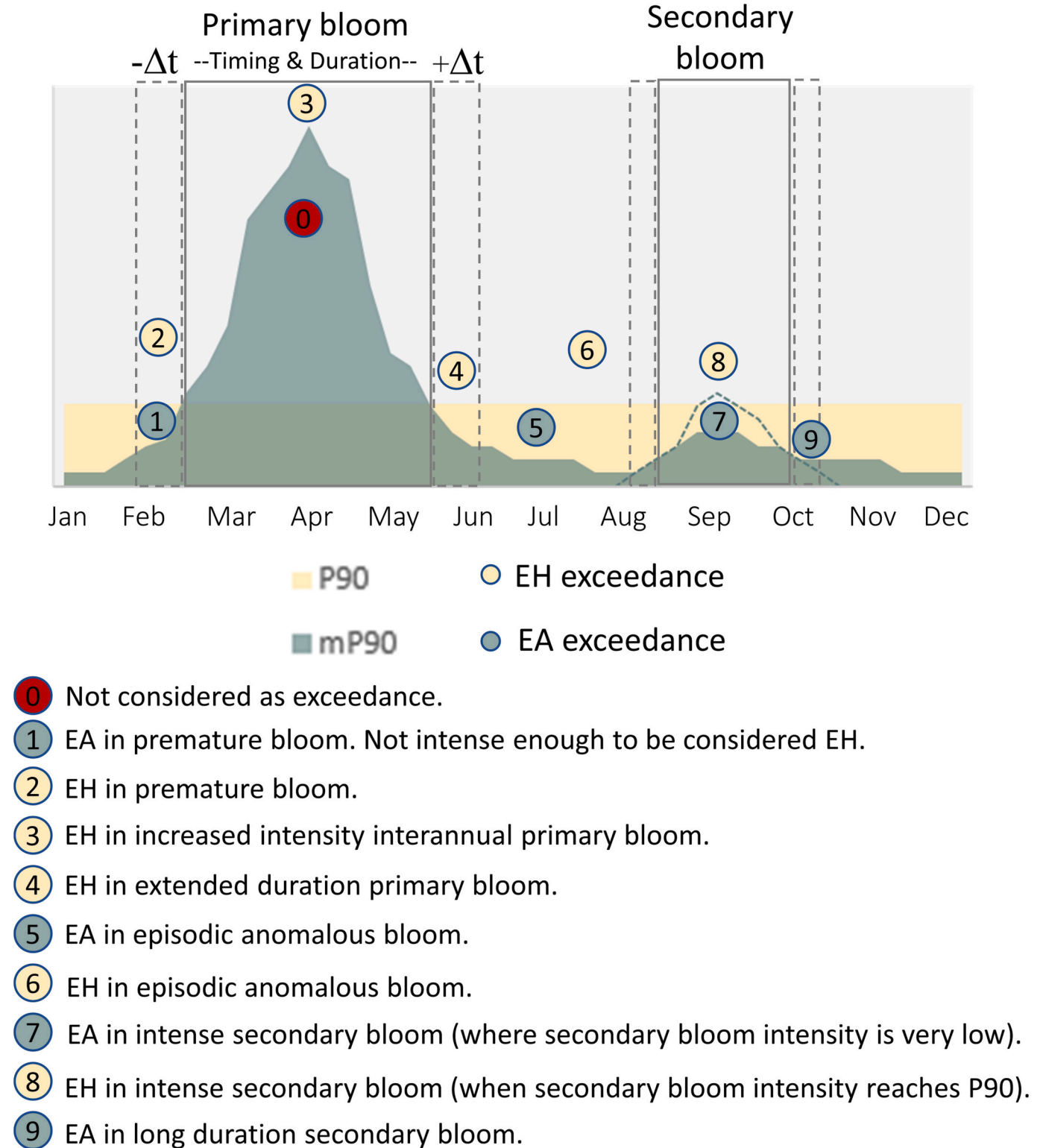


Fig. 10. Examples of Extreme highest (EH) and Extreme anomalous (EA) exceedance cases and their possible ecological meaning. P90: 90th percentile; mP90: monthly 90th percentile.

production and nutrients (Poikane et al., 2019).

The seasonal pattern found in the top 10% of the highest chlorophyll-a values, evidence that, at this threshold level, these extremes are still linked to the phytoplankton bloom dynamics and phenology. Other studies that analyze higher extremes like those based on the generalized extreme value distribution fitted to annual maxima (Britten, 2022) or the “Extreme Event waves” indices based on the 99th percentile (Di Biagio et al., 2020), find weaker patterns and trends, as more “rare” events. Di Biagio et al. (2020) also evidenced a significative influence of the retained threshold on the derived indices results. In this study, no comparative analysis has been attempted using other threshold limits such as 95th and 99th percentiles (although interesting to attempt in the future), because of our specific interest in analyzing the of 90th percentile exceedances distribution which is currently the most broadly used reference for water quality and phytoplankton ecological status assessments in European waters (European Commission, 2018).

The utility of considering the mP90 in the definition of the EH and EA extreme indicators, allows to account for the extreme values of chlorophyll-a produced during lower growing seasons (González Taboada and Anadón, 2014; Di Biagio et al., 2020), and to reject those that although high in magnitude ($> P90$) are among the seasonally expected values ($< mP90$).

The conceptual ecological/phenological meaning of the two complementary and non-overlapping EH and EA extreme indices is presented in Fig. 10. Overall, EH exceedances are mostly registered during the interannual growing season(s), and EA exceedances are found during low phytoplankton growing periods. EA exceedances may reflect unexpected episodic anomalous blooms, extreme values occurring during low intensity secondary seasonal blooms, or extremes registered earlier or later than the expected growing season timing. In the areas where the secondary bloom's magnitudes are sufficiently high (mP90 higher or close to P90), the extreme values associated with this bloom will likely fall under the EH indicator. Unexpected anomalous blooms can also be recorded as EH if their intensity overpasses the overall P90.

Another relevant aspect acknowledged in this study, is the need of integrating the spatio-temporal differences of the number of observations available throughout the area of study to normalize the count of extreme occurrences across different locations and times. In this sense, although the use of satellite imagery greatly increases the number of observations of chlorophyll-a, there are still locations and months with scarce or no observations. In these cases, as previously warned in Cole et al. (2012), the values of statistical indices such as the 90th percentiles, can entail significant uncertainty. Besides, in areas with low number of observations the probability of missing extreme values events, that usually have short durations, is not negligible. A workaround of this problem could be the use of reconstructed or merged products issued from satellite observations (Coppini et al., 2013; Sathyendranath et al., 2020; Staehr et al., 2022) or the use of model simulated chlorophyll-a (Henson et al., 2018; Miladinova et al., 2020; Di Biagio et al., 2020). However, these products also include uncertainty levels linked to the gap filling and modelling methods used, and the conclusions may be data-dependent (Henson et al., 2018).

The EH and EA extremes indicators approach, as per its ecological/phenological linkages, may help to narrow the search of possible causes behind these different events: i.e. phenology shifts of different seasonal blooms due to large scale climate change or local interannual Oceanometeorological variability (Ueyama and Monger, 2005; Sydesman and Bograd, 2009; Zhang et al., 2017; Henson et al., 2018; Cresswell-Clay et al., 2022), changes of ecosystem structures and successions, local scale episodic extreme events, either natural (i.e. large precipitations, volcanic eruptions, dust storms, upwellings) or anthropogenic (i.e. nutrient discharges from agriculture, industries or urban waste). Often these events obey to a combination of different causes (Barale et al., 2008).

The occurrences of the %EH and %EA in each single location show a very patchy variability that makes it difficult to draw any conclusion,

but some patterns appear when aggregated in the total exceedances' maps, in the monthly maps and in the annual trend maps.

Spatially, EH seem to prevail in natural mesotrophic and eutrophic waters like the offshore Atlantic areas above 40–45°N, coastal and shelf areas, the Baltic Sea, and the northern Black Sea with the exception of the central North Sea and some areas in the Arctic Ocean (Greenland and Barents Sea). However, most of the EA are found in the natural oligotrophic waters like the Macaronesian subregion and the Mediterranean offshore areas. This seems to point out to a quite generalized increase of the intensity of the primary blooms in European eutrophic waters whilst the number of blooms produced off the growing seasons seems to be more frequently observed in oligotrophic areas. In this last case, the low climatological ranges of chlorophyll-a can also contribute to the EA prevalence as whenever there is an episode triggering chlorophyll-a production, the EA threshold might be more easily reached.

Although this study does not aim to address the identification of the factors behind the patterns identified, some information related to the phytoplankton production drivers, and the trends of the blooms' intensity and timing shifts in different European regional seas have been searched in the literature to evaluate their coherence with the %EH and %EA patterns:

- (i) In the Baltic Sea, %EH maxima in April and July coincide with the first diatom dominated bloom after ice melting and winter nutrient enrichment and the second cyanobacteria dominated bloom respectively (HELCOM, 2009; Klais et al., 2011; Kahru et al., 2020; Beltran-Perez and Waniek, 2022). Warmer periods registered in the Baltic (HELCOM, 2009; Meier et al., 2022) cause spring blooms to peak earlier, and summer blooms to be longer and reach higher abundance and biomass (Spilling and Lindström, 2008; Suikkanen et al., 2013; Tamelander et al., 2017; Beltran-Perez and Waniek, 2022). The increasing trends for both %EH and %EA in the Baltic Sea seem to corroborate these findings.
- (ii) In the Arctic Ocean, the warm and saline Atlantic water transported by the subpolar gyre to the Arctic Ocean (Barents Sea and Greenland Sea) has nearly doubled over the past decades (Dalpadado et al., 2012; Oziel et al., 2017) causing the decline in sea-ice extent and a high interannual variability of the sea-ice edge (Oziel et al., 2017). The sea-ice edge seems to exert a dominant control on a bi-modal pattern of the spatial distribution of primary production in these areas (Koul et al., 2022). This bimodality seems to appear in the spatial distribution of the P90, and the cumulative %EH and %EA in the area, although less evident in the trend maps. In the Barents Sea, years of shallower mixed layer driven by both calm waters and higher freshwater input keeps the phytoplankton in the euphotic zone, causing the spring bloom to start earlier and reach higher biomass, but it ends sooner due to the lack of nutrients upwelling from the deep (Koul et al., 2022). In the Norwegian Sea warmer waters are correlated to earlier and stronger blooms in most regions but with later and weaker blooms in the eastern Norwegian Sea (Koul et al., 2022). The predominance of %EH increasing trends in the Arctic seas seem to be aligned with these results. However, any conclusion from this area has to be handled with care due to the low number of observations available from this area.
- (iii) in the Atlantic Ocean, the latitudinal shift of the %EH peaks coincides with the timing of the first interannual bloom also reported by González Taboada and Anadón (2014). The highest values of %EA in these areas is found during the pre-bloom and post-bloom months in each location which seem to support the influence of inter annual variability of environmental factors, such as wind forcing, photosynthetically active radiation and sea surface temperature (González Taboada and Anadón, 2014) on the timing, intensity and duration of the primary seasonal bloom in these areas. The trends of %EH and %EA in the Atlantic Ocean

seem to be generally increasing with a similar spatial pattern detected by Zhang et al. (2017) for the 2002–2015 period, except in two latitudinal strips, one between 30°N and 40°N, and the second one just below the Scotland-Iceland Ridge. Both areas seem to coincide with transitional areas at the limits of the sub-polar Atlantic gyre with the sub-tropical gyre in the south, and with the Norwegian Sea gyre (Hátún et al., 2021) in the north. The North Atlantic gyres and their variation are known to play a vital role in transporting heat, salt, and nutrients throughout the ocean basin and on their ecological structure and dynamics (Hátún et al., 2009, 2016, 2017; Ghosh et al., 2023). In addition, in the northern Atlantic zones, Feng et al. (2014) suggested that besides physical effects (bottom-up), zooplankton grazing effects (top-down) has a significant influence to shape the seasonal phytoplankton dynamics.

- (iv) In the North Sea, %EH are dominant in spring and %EA are significant in summer. The %EA register a more clear increasing trend in line with the increasing trends of the duration and the intensity of the summer blooms observed by Silva et al. (2021). In the North Sea, despite the important decrease of nutrient inputs since the 1980s (Painting et al., 2013; Burson et al., 2016) there is still a high chlorophyll-a production in both coastal and open waters that several authors relate to climatic variability via sea surface temperature, stratification conditions, water transparency and changes in phytoplankton dynamics (Desmit et al., 2020).
- (v) In the Mediterranean Sea, the highest %EH appear in winter (December to March), and the %EA expand from May to November, with a clear prevalence of %EA over %EH in the total count of exceedances. The prevalence of %EA on %EH seem in line with a general decrease of average chlorophyll-a values in the annual and monthly means and a positive trend of chlorophyll-a anomalies reported by Barale et al. (2008) for the period 1998–2003. Salgado-Hernanz et al. (2019) also found several high frequency episodes (irregular variability) in the Mediterranean Sea during all seasons. Although both papers situate most of these anomalies at near-coastal hotspots, linked to continental runoff, intense winds, exchanges with adjacent seas (i.e., in Alboran and Northern Aegean Seas) and to a growing “biological dynamism” at these sites, the %EA counted in this study can be found in all the Mediterranean waters (coastal and offshore). The increasing trends of %EH prevail in the Adriatic Sea and in the Levantine-Aegean subregion and seem to coincide spatially with the increasing trend of the duration of the main phytoplankton bloom observed in the 1998–2014 phenological trend maps from Salgado-Hernanz et al. (2019). Decreasing trends of %EA prevail in the northwestern and central Mediterranean subregions. Similar trend patterns were observed by Coppini et al. (2013) in the summer (May–September) chlorophyll-a averages for the period 1998–2009. For more updated periods 1997–2021 and 2003–2020 (European Union-Copernicus Marine Service, 2020; El Hourany et al., 2021) the decreasing trends of annual averages of chlorophyll-a in most of the Mediterranean area is also detected.
- (vi) In the Black Sea, clear decreasing trends of both %EH and %EA are found in the northwestern coast and in the Azov Sea. In these areas a clear decreasing trend of bloom frequency was found by Yunev et al. (2022) between 1998 and 2018, consistent with the decreasing trend of nitrate inputs from the Danube River. This decrease is a continuation of the marked decrease in the number of exceptional blooms, and the shift towards larger diatom dominance of the phytoplankton community found between 1991 and 2000, after the intense eutrophication period (1983–1990) (Bodeanu et al., 2004; Stokal and Kroeze, 2012). In these areas, the initiation of spring and early summer blooms is related with the spring intensification of riverine nutrient inputs

and the establishment of the seasonal pycnocline. In autumn, high phytoplankton biomass and frequent blooms are observed when the pycnocline begins to break down and convective mixing of the water column and storm activity resuspend nutrients accumulated in bottom waters during the seasonal stratification.

In the open waters of the Black Sea, separated by the above mentioned ones by the Rim Current that acts as a dynamic barrier locking the Danube plume waters (Özsoy and Ünlüata, 1997), %EH prevail between October and March and %EA between April and September. According to Miladinova et al. (2020) the winter phytoplankton bloom, with a peak in February, is the most abundant seasonal bloom and is closely related to the “cold intermediate layer” dynamics and the nitrate lifting from the storage in winter. Spring/summer blooms increase in ‘warm’ years, when the Danube discharge is high, the abundance of mesoscale eddies in late summer–autumn spread nutrients and biological matter over the basin, or when the “cold intermediate layer” is weak (Miladinova et al., 2020). Yunev et al. (2021) also report on important blooms from July to September maintained by nitrogen fixation by large diatoms despite low nitrate transport. The modelled phytoplankton evolution between 1998 and 2017 (Miladinova et al., 2020) show increasing spring and summer blooms in these areas. In this study, localized increasing trends of EH are found in the eastern open Black Sea, while in the western half some spots of increasing EA appear.

Although these comparisons are rather generic and much finer analysis should be engaged to confirm the interpretation of the EH and EA patterns and bloom drivers in each area, undoubtedly these extreme indices are providing valid information on the occurrence patterns of chlorophyll-a extremes across all European Seas with a beginning of explanation about their production framework.

One of the main advantages of these two indices approach is its conceptual and calculation simplicity if compared with other more complex and sophisticated methods (Di Biagio et al., 2020; Britten, 2022).

However, it has some limitations. The first one relates with the uncertainties linked to the estimation of chlorophyll-a. Although the use of frequency-based metrics can palliate the problems of overestimation or underestimation of the estimated chlorophyll-a values when these biases are constant through different ranges, there might be important uncertainties and bias over areas where the estimations of chlorophyll-a are highly uncertain and erratic, especially in case-2 waters, where chlorophyll-a estimations can reach extremely high values influenced by non-covarying concentrations of suspended particulate matter and coloured dissolved organic matter (Lavigne et al., 2021), which should probably be filtered out as outliers.

Other important source of uncertainties is linked with the size and distribution of data gaps: even if the normalized metrics such as the percentages can mitigate the potential misinterpretations due to different sampling sizes across areas and seasons, these data gaps may also induce uncertainties and bias in the extreme metrics values and derived patterns, especially in areas and seasons with very low number of observations. In addition, because of their low frequency (<10%) extreme events (and their patterns) are more difficult to track with low sampling efforts.

These limitations could be overcome using datasets aiming at improved chlorophyll-a estimates and reduced data gaps, such as those generated under the ESA Ocean Color Climate Change Initiative (Sathyendranath et al., 2021), the Copernicus-GlobColour project (European Union-Copernicus Marine Service, 2022) or the updated ocean color v2022 reprocessing (<https://oceancolor.gsfc.nasa.gov/data/reprocessing/>) for global scales, or other regional datasets proposed for different European Seas (Brando et al., 2021; Suslin and Churilova, 2016; Lavigne et al., 2021).

Another limitation lies in the impossibility of EH and EA to clearly discern between the exceedances found in the pre-bloom and post bloom periods for both the primary and secondary annual blooms and the local

anomalous episodic events. These indices are also not able to discriminate extreme events leading to adverse impacts like for instance, eutrophication or toxic HABs episodes, as other impact-based indicators do by integrating the context of local exposure and vulnerability to these impacts (Ruane et al., 2022).

Despite these weaknesses, the EH and EA extremes indices counted during the 2003–2021 period evidence that both, areas with significant increasing trends and areas with significant decreasing trends of extreme chlorophyll-a occurrences are found across the European Seas. The areas affected with significant increasing trends are higher than those in which significant decreasing trends are observed. However, the significant decreasing trends are found in areas where important ecological issues were found in the late 20th century, indicating a positive recovery or reduction of eutrophication events due to management measures (Andersen et al., 2017; OSPAR Commission, 2017; Salgado-Hernanz et al., 2022). Overall, the EH and EA trends are reflecting the climate-driven physical, and ecological changes as well as the anthropogenic activities and measures that are affecting the European Seas.

In conclusion, this study provides a good basis for future work to i) validate the identification and counting of EH and EA extreme events by testing them against good quality in-situ time series of chlorophyll-a in different marine water types, ii) complement and/or compare these indices with others extreme indices or approaches and iii) promote a deeper analysis of the specific drivers of the extreme events identified to soundly support assessments and decision making.

Description of author's responsibilities

Yolanda Sagarminaga: Conception, acquisition and analysis of data, interpretation of results and manuscript redaction.

Angel Borja: Critical revision of analysis methods, outcomes and discussion of results, and manuscript redaction.

Almudena Fontán: Critical revision of analysis methods, outcomes and discussion of results, and manuscript redaction.

Funding

This work was funded by the European Environmental Agency, under the framework partnership agreement concerning the European Topic Centre on Inland, Coastal and Marine waters (2019–2022) No CP/EEA/NSS/18/002-ETC/ICM, and by GES4SEAS (Achieving Good Environmental Status for maintaining ecosystem services, by assessing integrated impacts of cumulative pressures) project, funded by the European Union under the Horizon Europe program (grant agreement no. 101059877), www.ges4seas.eu. This paper is contribution n° 1187 from AZTI, Marine Research, Basque Research and Technology Alliance (BRTA).

CRedit authorship contribution statement

Yolanda Sagarminaga: Conceptualization, Methodology, Formal analysis, Investigation, Writing – original draft, Writing – review & editing. **Angel Borja:** Validation, Writing – review & editing, Supervision, Project administration, Funding acquisition. **Almudena Fontán:** Validation, Writing – review & editing.

Declaration of Competing Interest

The authors declare that they have no known competing financial interests or personal relationships that could have appeared to influence the work reported in this paper.

Data availability

The data used and generated in this study are publicly available: MODIS-AQUA v2018; doi:10.5067/AQUA/MODIS/L3M/CHL/2018.

Sagarminaga Y.(2023).<https://doi.org/10.5281/zenodo.7839643>

Appendix A. Supplementary data

Supplementary data to this article can be found online at <https://doi.org/10.1016/j.rse.2023.113885>.

References

- Andersen, J.H., Carstensen, J., Conley, D.J., Dromph, K., Fleming-Lehtinen, V., Gustafsson, B.G., Josefson, A.B., Norkko, A., Villnäs, A., Murray, C., 2017. Long-term temporal and spatial trends in eutrophication status of the Baltic Sea: eutrophication in the Baltic Sea. *Biol. Rev.* 92 (1), 135–149. <https://doi.org/10.1111/brv.12221>.
- Bailey, L.D., Van de Pol, M., 2016. Tackling extremes: challenges for ecological and evolutionary research on extreme climatic events. *J. Anim. Ecol.* 85, 85–96. <https://doi.org/10.1111/1365-2656.12451>.
- Barale, V., Jaquet, J.-M., Ndiaye, M., 2008. Algal blooming patterns and anomalies in the Mediterranean Sea as derived from the SeaWiFS data set (1998–2003). *Remote Sens. Environ.* 112 (8), 3300–3313. <https://doi.org/10.1016/j.rse.2007.10.014>.
- Beltran-Perez, O.D., Waniek, J.J., 2022. Inter-annual variability of spring and summer blooms in the eastern Baltic Sea. *Front. Mar. Sci.* 9, 928633. <https://doi.org/10.3389/fmars.2022.928633>.
- Berdalet, E., Fleming, L.E., Gowen, R., Davidson, K., Hess, P., Backer, L.C., et al., 2015. Marine harmful algal blooms, human health and well-being: challenges and opportunities in the 21st century. *J. Mar. Biol. Assoc. United Kingdom* 96, 61–91. <https://doi.org/10.1017/s0025315415001733>.
- Bivand, R., Keitt, T., Rowlingson, B., Pebesma, E., Sumner, M., Hijmans, R., 2015. Package 'rgdal'. Bindings for the Geospatial Data Abstraction Library. Available online: <https://cran.r-project.org/web/packages/rgdal/index.html>.
- Bodeanu, N., Andrei, C., Boicenco, L., Popa, L., Sburlea, A., 2004. A new trend of the phytoplankton structure and dynamics in the Romanian marine waters. *Cercetari Marine* 35. https://www.researchgate.net/publication/266870913_A_new_trend_of_the_phytoplankton_structure_and_dynamics_in_the_Romanian_marine_waters.
- Borja, A., Elliott, M., Carstensen, J., Heiskanen, A.S., Van de Bund, W., 2010. Marine management – towards an integrated implementation of the European Marine Strategy Framework and the Water Framework Directives. *Mar. Pollut. Bull.* 60, 2175–2186.
- Borja, A., Garmendia, J.M., Menchaca, I., Uriarte, A., Sagarminaga, Y., 2019. Yes, we can! Large-scale integrative assessment of European regional seas, using open access databases. *Front. Mar. Sci.* 6. <https://doi.org/10.3389/fmars.2019.00019>.
- Brando, V.E., Sammartino, M., Colella, S., Bracaglia, M., Di Cicco, A., D'Alimonte, D., Kajiyama, T., Kaitala, S., Attila, J., 2021. Phytoplankton bloom dynamics in the Baltic Sea using a consistently reprocessed time series of multi-sensor reflectance and novel chlorophyll-a retrievals. *Remote Sens.* 13 (16), 3071. <https://doi.org/10.3390/rs13163071>.
- Britten, G.L., 2022. Extreme value distributions describe interannual variability in the seasonal North Atlantic phytoplankton bloom. *Limnol. Oceanogr. Lett.* 7 (3), 269–276. <https://doi.org/10.1002/lol2.10247>.
- Burson, A., Stomp, M., Akil, L., Brussaard, C.P.D., Huisman, J., 2016. Unbalanced reduction of nutrient loads has created an offshore gradient from phosphorus to nitrogen limitation in the North Sea. *Limnol. Oceanogr.* 61 (3), 869–888. <https://doi.org/10.1002/lno.10257>.
- Cloern, J.E., 2001. Our evolving conceptual model of the coastal eutrophication problem. *Mar. Ecol. Prog. Ser.* 210, 223–253.
- Cole, H., Henson, S., Martin, A., Yool, A., 2012. Mind the gap: the impact of missing data on the calculation of phytoplankton phenology metrics: impact of data gaps on phenology metrics. *J. Geophys. Res. Oceans* 117 (C8), n/a–n/a. <https://doi.org/10.1029/2012JC008249>.
- Coles, S., 2001. An Introduction to Statistical Modeling of Extreme Values. Springer, London. <https://doi.org/10.1007/978-1-4471-3675-0>.
- Coppini, G., Lyubartsev, V., Pinardi, N., Colella, S., Santoleri, R., Christiansen, T., 2013. The use of ocean-colour data to estimate Chl-a trends in European seas. *Int. J. Geosci.* 04 (06), 927–949. <https://doi.org/10.4236/ijg.2013.46087>.
- Cresswell-Clay, N., Ummenhofer, C.C., Thatcher, D.L., Wanamaker, A.D., Denniston, R. F., Asmerom, Y., Polyak, V.J., 2022. Twentieth-century Azores high expansion unprecedented in the past 1,200 years. *Nat. Geosci.* 15 (7), 548–553. <https://doi.org/10.1038/s41561-022-00971-w>.
- Dalpadado, P., Ingvaldsen, R.B., Stige, L.C., Bogstad, B., Knutsen, T., Ottersen, G., Ellertsen, B., 2012. Climate effects on Barents Sea ecosystem dynamics. *ICES J. Mar. Sci.* 69 (7), 1303–1316. <https://doi.org/10.1093/icesjms/fss063>.
- Deckmyn, A., 2018. Package Mapdata: Supplement to Maps Package, Providing the Larger and/or Higher-Resolution Databases. <https://CRAN.R-project.org/package=mapdata>.
- Deckmyn, A., 2021. Package Maps: Display of maps. Projection code and larger maps are in separate packages ('mapproj' and 'mapdata'). <https://CRAN.R-project.org/package=maps>.
- Desmit, X., Nohe, A., Borges, A.V., Prins, T., De Cauwer, K., Lagring, R., Van Der Zande, D., Sabbe, K., 2020. Changes in chlorophyll concentration and phenology in the North Sea in relation to de-eutrophication and sea surface warming. *Limnol. Oceanogr.* 65 (4), 828–847. <https://doi.org/10.1002/lno.11351>.
- Di Biagio, V., 2016. A method to characterize statistical extremes in marine biogeochemistry: the case of Mediterranean chlorophyll. PhD. Università degli studi di Trieste. Scienze della terra e meccanica dei fluidi.

- Di Biagio, V., Cossarini, G., Salon, S., Solidoro, C., 2020. Extreme event waves in marine ecosystems: an application to Mediterranean Sea surface chlorophyll. *Biogeosciences* 17 (23), 5967–5988. <https://doi.org/10.5194/bg-17-5967-2020>.
- El Hourany, R., Mejia, C., Faour, G., Crépon, M., Thiria, S., 2021. Evidencing the impact of climate change on the phytoplankton community of the Mediterranean Sea through a bioregionalization approach. *J. Geophys. Res. Oceans* 126 (4). <https://doi.org/10.1029/2020JC016808>.
- Environmental European Agency, 2019. Nutrient enrichment and eutrophication in Europe's seas. EEA Report No 14/2019, ISBN 978-92-9480-111-1. <https://doi.org/10.2800/092643>. ISSN 1977-8449.
- Environmental European Agency, 2022. Regional seas around Europe. Prod-ID: DAT-208-en Created 24 Oct 2022. <https://www.eea.europa.eu/data-and-maps/data/europe-seas-2>.
- European Commission, 2018. Establishing, pursuant to Directive 2000/60/EC of the European Parliament and of the Council, the values of the Member State monitoring system classifications as a result of the intercalibration exercise and repealing Commission Decision 2013/480/EU. Commission Decision 2018/229/EU. <https://eur-lex.europa.eu/legal-content/EN/TXT/PDF/?uri=CELEX:32018D0229&from=HU2000/60/EC>.
- European Union-Copernicus Marine Service, 2020. Mediterranean Sea chlorophyll-a trend map from observations reprocessing. Mercator Ocean Int. <https://doi.org/10.48670/MOI-00260>.
- European Union-Copernicus Marine Service, 2022. Global Ocean Colour (Copernicus-GlobColour), Bio-Geo-Chemical, L3 (daily) from Satellite Observations (1997-ongoing). Mercator Ocean International. <https://doi.org/10.48670/MOI-00280>.
- Feng, J., Stige, L.C., Durant, J.M., Hessen, D.O., Zhu, L., Hjermann, D.O., Llope, M., Stenseth, N.C., 2014. Large-scale season-dependent effects of temperature and zooplankton on phytoplankton in the North Atlantic. *Mar. Ecol. Prog. Ser.* 502, 25–37. <https://doi.org/10.3354/meps10724>.
- Ferreira, J.G., Andersen, J.H., Borja, A., Bricker, S.B., Camp, J., Cardoso da Silva, M., Garcés, E., Heiskanen, A.-S., Humborg, C., Ignatiadis, L., Lancelot, C., Menesguen, A., Tett, P., Hoepffner, N., Claussen, U., 2011. Overview of eutrophication indicators to assess environmental status within the European Marine Strategy Framework Directive. *Estuar. Coast. Shelf Sci.* 93 (2), 117–131. <https://doi.org/10.1016/j.ecss.2011.03.014>.
- Franz, B.A., Bailey, S.W., Eplee Jr., R.E., Lee, S., Patt, F.S., Gerhard, M., 2018. NASA Multi-Mission Ocean Color Reprocessing 2018.0. *Proc. Ocean Optics* 2018, Dubrovnik, Croatia, 8–12 October 2018. https://2018.oceanopticsconference.org/extended/Franz_Bryan.pdf.
- Ghosh, R., Putrasahan, D., Manzini, E., Lohmann, K., Keil, P., Hand, R., Bader, J., Matei, D., Jungclaus, J.H., 2023. Two distinct phases of North Atlantic eastern subpolar gyre and warming hole evolution under global warming. *J. Clim.* 36 (6), 1881–1894. <https://doi.org/10.1175/JCLI-D-22-0222.1>.
- Gilbert, R.O., 1987. *Statistical Methods for Environmental Pollution Monitoring*. Van Nostrand Reinhold, New York.
- Gilbert, P.M., Berdalet, E., Burford, M.A., Pitcher, G.C., Zhou, M., 2018. Introduction to the global ecology and oceanography of harmful algal blooms (GEOHAB) synthesis. In: Gilbert, P.M., Berdalet, E., Burford, M.A., Pitcher, G.C., Zhou, M. (Eds.), *Global Ecology and Oceanography of Harmful Algal Blooms*, vol. 232. Springer International Publishing, pp. 3–7. https://doi.org/10.1007/978-3-319-70069-4_1.
- Gohin, F., Saulquin, B., Oger-Jeanneret, H., Lozac'h, L., Lampert, L., Lefebvre, A., Riou, P., Bruchon, F., 2008. Towards a better assessment of the ecological status of coastal waters using satellite-derived chlorophyll-a concentrations. *Remote Sens. Environ.* 112 (8), 3329–3340. <https://doi.org/10.1016/j.rse.2008.02.014>.
- Gómez-Jakobsen, F., Ferrera, I., Yebra, L., Mercado, J.M., 2022. Two decades of satellite surface chlorophyll a concentration (1998–2019) in the Spanish Mediterranean marine waters (Western Mediterranean Sea): Trends, phenology and eutrophication assessment. *Remote Sensing Applications: Society and Environment* 28, 100855. <https://doi.org/10.1016/j.rsase.2022.100855>.
- González Taboada, F., Anadón, R., 2014. Seasonality of North Atlantic phytoplankton from space: impact of environmental forcing on a changing phenology (1998–2012). *Glob. Chang. Biol.* 20 (3), 698–712. <https://doi.org/10.1111/gcb.12352>.
- Gutschick, V.P., BassiriRad, H., 2003. Extreme events as shaping physiology, ecology, and evolution of plants: toward a unified definition and evaluation of their consequences. *New Phytol.* 160 (1), 21–42. <https://doi.org/10.1046/j.1469-8137.2003.00866.x>.
- Hátún, H., Payne, M.R., Beaugrand, G., Reid, P.C., Sandø, A.B., Drange, H., Hansen, B., Jacobsen, J.A., Bloch, D., 2009. Large bio-geographical shifts in the North-Eastern Atlantic Ocean: from the subpolar gyre, via plankton, to blue whiting and pilot whales. *Prog. Oceanogr.* 80 (3–4), 149–162. <https://doi.org/10.1016/j.pocean.2009.03.001>.
- Hátún, H., Lohmann, K., Matei, D., Jungclaus, J.H., Pacariz, S., Bersch, M., Gislason, A., Ólafsson, J., Reid, P.C., 2016. An inflated subpolar gyre blows life toward the northeastern Atlantic. *Prog. Oceanogr.* 147, 49–66. <https://doi.org/10.1016/j.pocean.2016.07.009>.
- Hátún, H., Azetsu-Scott, K., Somavilla, R., Rey, F., Johnson, C., Mathis, M., Mikolajewicz, U., Coupel, P., Tremblay, J.-É., Hartman, S., Pacariz, S.V., Salter, I., Ólafsson, J., 2017. The subpolar gyre regulates silicate concentrations in the North Atlantic. *Sci. Rep.* 7 (1), 14576. <https://doi.org/10.1038/s41598-017-14837-4>.
- Hátún, H., Chaffik, L., Larsen, K.M.H., 2021. The Norwegian Sea gyre – a regulator of Iceland-Scotland ridge exchanges. *Front. Mar. Sci.* 8 <https://doi.org/10.3389/fmars.2021.694614>.
- HELCOM, 2009. Eutrophication in the Baltic Sea – An Integrated Thematic Assessment of the Effects of Nutrient Enrichment and Eutrophication in the Baltic Sea Region. *Balt Sea Environ. Proc. No.* 115B.
- Henson, S.A., Cole, H.S., Hopkins, J., Martin, A.P., Yool, A., 2018. Detection of climate change-driven trends in phytoplankton phenology. *Glob. Chang. Biol.* 24 (1), e101–e111. <https://doi.org/10.1111/gcb.13886>.
- Hijmans, R.J., Van Etten, J., 2012. Package raster: geographic analysis and modeling with raster data. R package version 2.0-12. <http://CRAN.R-project.org/package=raster>.
- Hu, C., Lee, Z., Franz, B., 2012. Chlorophyll a algorithms for oligotrophic oceans: A novel approach based on three-band reflectance difference. *J. Geophys. Res.* 117 (C1). <https://doi.org/10.1029/2011jc007395>.
- Hu, C., Feng, L., Lee, Z., Franz, B.A., Bailey, S.W., Werdell, P.J., Proctor, C.W., 2019. Improving satellite global chlorophyll a data products through algorithm refinement and data recovery. *J. Geophys. Res. Oceans* 124 (3), 1524–1543. <https://doi.org/10.1029/2019JC014941>.
- IPCC, 2012. In: Field, C.B., Barros, V., Stocker, T.F., Qin, D., Dokken, D.J., Ebi, K.L., Mastrandrea, M.D., Mach, K.J., Plattner, G.-K., Allen, S.K., Tignor, M., Midgley, P.M. (Eds.), *Managing the Risks of Extreme Events and Disasters to Advance Climate Change Adaptation. A Special Report of Working Groups I and II of the Intergovernmental Panel on Climate Change*. Cambridge University Press, Cambridge, UK, and New York, NY, USA, 582 pp. https://www.ipcc.ch/site/assets/uploads/2018/03/SREX_Full_Report-1.pdf.
- IPCC, 2022a. In: Pörtner, H.-O., Roberts, D.C., Masson-Delmotte, V., Zhai, P., Tignor, M., Poloczanska, E., Mintenbeck, K., Alegria, A., Nicolai, M., Okem, A., Petzold, J., Rama, B., Weyer, N.M. (Eds.), *IPCC Special Report on the Ocean and Cryosphere in a Changing Climate*. Cambridge University Press, Cambridge, UK and New York, NY, USA, 755 pp.
- IPCC, 2022b. In: Pörtner, H.-O., Roberts, D.C., Tignor, M., Poloczanska, E.S., Mintenbeck, K., Alegria, A., Craig, M., Langsdorf, S., Löschke, S., Möller, V., Okem, A., Rama, B. (Eds.), *Climate Change 2022: Impacts, Adaptation and Vulnerability. Contribution of Working Group II to the Sixth Assessment Report of the Intergovernmental Panel on Climate Change*. Cambridge University Press, Cambridge, UK and New York, NY, USA. <https://doi.org/10.1017/9781009325844>, 3056 pp.
- Kahru, M., Elmgren, R., Kaiser, J., Wasmund, N., Savchuk, O., 2020. Cyanobacterial blooms in the Baltic Sea: correlations with environmental factors. *Harmful Algae* 92, 101739. <https://doi.org/10.1016/j.hal.2019.101739>.
- Kendall, M.G., 1975. *Rank Correlation Methods*, 4th ed. Charles Griffin, London.
- Kinnison, R.R., 1983. *Applied extreme-value statistics*. United States. <https://doi.org/10.2172/6045789>.
- Klais, R., Tamminen, T., Kremp, A., Spilling, K., Olli, K., 2011. Decadal-scale changes of dinoflagellates and diatoms in the anomalous Baltic Sea spring bloom. *PLoS One* 6 (6), e21567. <https://doi.org/10.1371/journal.pone.0021567>.
- Koul, V., Brune, S., Baehr, J., Schrum, C., 2022. Impact of decadal trends in the surface climate of the North Atlantic subpolar gyre on the marine environment of the Barents Sea. *Front. Mar. Sci.* 8 <https://doi.org/10.3389/fmars.2021.778335>.
- Lavigne, H., Van der Zande, D., Ruddick, K., Cardoso Dos Santos, J.F., Gohin, F., Brotas, V., Kratzer, S., 2021. Quality-control tests for OC4, OC5 and NIR-red satellite chlorophyll-a algorithms applied to coastal waters. *Remote Sens. Environ.* 255, 112237. <https://doi.org/10.1016/j.rse.2020.112237>.
- Lewin-Koh, J.N., Bivand, R., 2011. *Package Maptools: Tools for Reading and Handling Spatial Objects*. R Package Version 0.8–10.
- Longhurst, A.R., 2007. Chapter 7 - Provinces: the secondary compartments. In: Longhurst, A.R. (Ed.), *Ecological Geography of the Sea*, Second edition. Academic Press, pp. 103–114. <https://doi.org/10.1016/B978-0-12455521-1/50008-5>.
- Macias Moy, D., Friedland, R., Stips, A., Miladinova-Marinova, S., Pam, O., Garcia Gorriz, E., Melin, F., 2020. Applying the marine modelling framework to estimate primary production in EU marine waters. EUR 30546 EN, Publications Office of the European Union, Luxembourg. ISBN 978-92-76-27860-3, JRC122600. <https://doi.org/10.2760/19851>.
- Maritorena, S., Fanton d'Andon, O., Hembise, Mangin, A., Siegel, D.A., 2010. Merged satellite ocean color data products using a bio-optical model: characteristics, benefits and issues. *Remote Sens. Environ.* 114 (8), 1791–1804.
- Meier, H.E.M., Kniesbusch, M., Dieterich, C., Gröger, M., Zorita, E., Elmgren, R., Myrberg, K., Ahola, M.P., Bartosova, A., Bonsdorff, E., Börgel, F., Capell, R., Carlén, I., Carlund, T., Carstensen, J., Christensen, O.B., Dierschke, V., Frauen, C., Frederiksen, M., Zhang, W., 2022. Climate change in the Baltic Sea region: a summary. *Earth Syst. Dynam.* 13 (1), 457–593. <https://doi.org/10.5194/esd-13-457-2022>.
- Miladinova, S., Stips, A., Macias Moy, D., Garcia-Goriz, E., 2020. Seasonal and inter-annual variability of the phytoplankton dynamics in the Black Sea Inner Basin. *Oceans* 1 (4), 251–273. <https://doi.org/10.3390/oceans1040018>.
- Morozov, E., Korosov, A., Pozdnyakov, D., Pettersson, L., Sychev, V., 2010. A new area-specific bio-optical algorithm for the Bay of Biscay and assessment of its potential for SeaWiFS and MODIS/aqua data merging. *Int. J. Remote Sens.* 31 (24), 6541–6565. <https://doi.org/10.1080/01431161.2010.508802>.
- NASA-Ocean Biology Processing Group, 2018. Moderate-Resolution Imaging Spectroradiometer (MODIS) Aqua Chlorophyll Data; 2018 Reprocessing. NASA OB DAAC, Greenbelt, MD, USA. <https://doi.org/10.5067/AQUA/MODIS/L3M/CHL/2018>. Accessed on 01/12/2021.
- Novoa, S., Chust, G., Sagarmínaga, Y., Revilla, M., Borja, A., Franco, J., 2012. Water quality assessment using satellite-derived chlorophyll-a within the European directives, in the southeastern Bay of Biscay. *Mar. Pollut. Bull.* 64 (4), 739–750. ISSN 0025-326X. <https://doi.org/10.1016/j.marpolbul.2012.01.020>.
- O'Reilly, J.E., Werdell, P.J., 2019. Chlorophyll algorithms for ocean color sensors - OC4, OC5 & OC6. *Remote Sens. Environ.* 229, 32–47. <https://doi.org/10.1016/j.rse.2019.04.021>.

- O'Reilly, J.E., Maritorena, S., O'Brien, M.C., Siegel, D.A., Toole, D., Menzies, D., Culver, M., 2000. Volume 11, SeaWiFS postlaunch calibration and validation analyses (Vol. 11), part 3. Tech. Rep. NASA Technical Memorandum 2000-206892.
- OSPAR Commission, 2017. Eutrophication Status of the OSPAR Maritime Area Third Integrated Report on the Eutrophication Status of the OSPAR Maritime Area. ISBN: 978-1-911458-34-0 Publication Number: 694/2017.
- Oziel, L., Neukermans, G., Ardyna, M., Lancelot, C., Tison, J.-L., Wassmann, P., Sirven, J., Ruiz-Pino, D., Gascard, J.-C., 2017. Role for Atlantic inflows and sea ice loss on shifting phytoplankton blooms in the Barents Sea: SHIFTING BLOOMS IN THE BARENTS SEA. *J. Geophys. Res. Oceans* 122 (6), 5121–5139. <https://doi.org/10.1002/2016JC012582>.
- Özsoy, E., Ünlüata, Ü., 1997. Oceanography of the Black Sea: a review of some recent results. *Earth Sci. Rev.* 42 (4), 231–272. [https://doi.org/10.1016/S0012-8252\(97\)81859-4](https://doi.org/10.1016/S0012-8252(97)81859-4).
- Painting, S., Foden, R., Forster, R., Van Der Molen, J., Aldridge, J., Best, M., Jonas, P., Hydes, D., Walshaw, P., Webster, L., Gubbins, M., Heath, M., McGovern, E., Vincent, C., Gowen, R., O'Boyle, S., 2013. Impacts of climate change on nutrient enrichment. *MCCIP Sci. Rev.* 2013 <https://doi.org/10.14465/2013.ARC23.219-235>, 17 pages.
- Perpinán, O., Hijmans, R., 2022. rasterVis. R package version 0.51.2. <https://oscarperpinan.github.io/rastervis/>.
- Pierce, D., 2021. Package ncd4f: Interface to Unidata netCDF (Version 4 or Earlier) Format Data Files (ncdf4 v1.19). License GPL (>= 3). <http://cirrus.ucsd.edu/~pie/ncdf/>.
- Pitarch, J., Volpe, G., Colella, S., Krasemann, H., Santoleri, R., 2016. Remote sensing of chlorophyll in the Baltic Sea at basin scale from 1997 to 2012 using merged multisensor data. *Ocean Sci.* 12 (2), 379–389. <https://doi.org/10.5194/os-12-379-2016>.
- Pohlert, T., 2020. Package trend: Non-Parametric Trend Tests and Change-Point Detection. <https://CRAN.R-project.org/package=trend>.
- Poikane, S., Kelly, M.G., Salas Herrero, F., Pitt, J.-A., Jarvie, H.P., Claussen, U., Leujak, W., Lyche Solheim, A., Teixeira, H., Phillips, G., 2019. Nutrient criteria for surface waters under the European Water Framework Directive: current state-of-the-art, challenges and future outlook. *Sci. Total Environ.* 695, 133888 <https://doi.org/10.1016/j.scitotenv.2019.133888>.
- QGIS.org, 2022. QGIS Geographic Information System. QGIS Association. <http://www.qgis.org>.
- R Core Team, 2020. R: A Language and Environment for Statistical Computing. R Foundation for Statistical Computing, Vienna, Austria. <https://www.R-project.org/>.
- Ren, F.-M., Trewin, B., et al., 2018. A research progress review on regional extreme events. *Adv. Clim. Chang. Res.* 9 (3), 161–169.
- Reygondeau, G., Longhurst, A., Martinez, E., Beaugrand, G., Antoine, D., Maury, O., 2013. Dynamic biogeochemical provinces in the global ocean: DYNAMIC BIOGEOCHEMICAL PROVINCES. *Glob. Biogeochem. Cycles* 27 (4), 1046–1058. <https://doi.org/10.1002/gbc.20089>.
- RStudio Team, 2019. RStudio: Integrated Development for R. RStudio, Inc., Boston, MA. <http://www.rstudio.com/>.
- Ruane, A.C., Vautard, R., Ranasinghe, R., Sillmann, J., Coppola, E., Arnell, N., Cruz, F.A., Dessai, S., Iles, C.E., Islam, A.K.M.S., Jones, R.G., Rahimi, M., Carrascal, D.R., Seneviratne, S.I., Servonnat, J., Sörensson, A.A., Sylla, M.B., Tebaldi, C., Wang, W., Zaaboul, R., 2022. The climatic impact-driver framework for assessment of risk-relevant climate information. *Earth's Future* 10 (11). <https://doi.org/10.1029/2022EF002803>.
- Sagarminaga, Y., 2023. Extreme values and exceedances of chlorophyll-a calculated from the OBPG MODIS AQUA v2018 dataset's daily files in European seas between 2003 and 2021. (1.0) [data set]. Zenodo. <https://doi.org/10.5281/zenodo.7839643>.
- Salgado-Hernanz, P.M., Racault, M.-F., Font-Muñoz, J.S., Basterretxea, G., 2019. Trends in phytoplankton phenology in the Mediterranean Sea based on ocean-colour remote sensing. *Remote Sens. Environ.* 221, 50–64. <https://doi.org/10.1016/j.rse.2018.10.036>.
- Salgado-Hernanz, P.M., Regaudie-de-Gioux, A., Antoine, D., Basterretxea, G., 2022. Pelagic primary production in the coastal Mediterranean Sea: variability, trends, and contribution to basin-scale budgets. *Biogeosciences* 19 (1), 47–69. <https://doi.org/10.5194/bg-19-47-2022>.
- Sanseverino, I., Conduto, D., Pozzoli, L., Dobricic, S., Lettieri, T., 2016. Algal bloom and its economic impact (EUR 27905 EN. JRC Technical Report, 52 pp. ISBN 978-92-79-58101-4). JRC.
- Sarkar, D., 2008. Lattice: Multivariate Data Visualization with R. Springer, New York. ISBN 978-0-387-75968-5. <http://lmdvr.r-forge.r-project.org>.
- Sarkar, D., Andrews, F., 2019. Package latticeExtra: Extra Graphical Utilities Based on Lattice. <https://CRAN.R-project.org/package=latticeExtra>.
- Sathyendranath, S., Brewin, R.J.W., Jackson, T., Mélin, F., Platt, T., 2017. Ocean-colour products for climate-change studies: What are their ideal characteristics? *Remote Sens. Environ.* 203, 125–138. <https://doi.org/10.1016/j.rse.2017.04.017>.
- Sathyendranath, S., Jackson, T., Brockmann, C., Brotas, V., Calton, B., Chuprin, A., Clements, O., Cipollini, P., Danne, O., Dingle, J., Donlon, C., Grant, M., Groom, S., Krasemann, H., Lavender, S., Mazeran, C., Mélin, F., Moore, T.S., Müller, D., Regner, P., Steinmetz, F., Steele, C., Swinton, J., Valente, A., Zühlke, M., Feldman, G., Franz, B., Frouin, R., Werdell, J., Platt, T., 2020. ESA Ocean Colour Climate Change Initiative (Ocean Colour_cci): Global chlorophyll-a data products gridded on a sinusoidal projection, Version 4.2. Centre for Environmental Data Analysis. <https://catalogue.ceda.ac.uk/uuid/99348189bd33459cbd597a58c30d8d10>.
- Sathyendranath, S., Jackson, T., Brockmann, C., Brotas, V., Calton, B., Chuprin, A., Clements, O., Cipollini, P., Danne, O., Dingle, J., Donlon, C., Grant, M., Groom, S., Krasemann, H., Lavender, S., Mazeran, C., Mélin, F., Müller, D., Steinmetz, F., Platt, T., 2021. ESA Ocean Colour Climate Change Initiative (Ocean Colour_cci): Version 5.0 Data. NERC EDS Centre for Environmental Data Analysis. <https://doi.org/10.5285/1DBE7A109C0244AAD713E078FD3059A>.
- Schulzweida, U., 2021. CDO User Guide (Version 2.0.0). Zenodo. <https://doi.org/10.5281/zenodo.5614769>.
- Sen, P., 1968. Estimated of the regression coefficient based on Kendall's Tau. *J. Am. Stat. Assoc.* 39, 1379–1389.
- Silva, E., Counillon, F., Brajard, J., Korosov, A., Pettersson, L.H., Samuelsen, A., Keenlyside, N., 2021. Twenty-one years of phytoplankton bloom phenology in the Barents, Norwegian, and north seas. *Front. Mar. Sci.* 8 <https://doi.org/10.3389/fmars.2021.746327>.
- Smith, M.D., 2011. An ecological perspective on extreme climatic events: a synthetic definition and framework to guide future research. *J. Ecol.* 99 (3), 656–663.
- Spilling, K., Lindström, M., 2008. Phytoplankton life cycle transformations lead to species-specific effects on sediment processes in the Baltic Sea. *Cont. Shelf Res.* 28 (17), 2488–2495. <https://doi.org/10.1016/j.csr.2008.07.004>.
- Staehr, S.U., Van der Zande, D., Staehr, P.A.U., Markager, S., 2022. Suitability of multisensory satellites for long-term chlorophyll assessment in coastal waters: A case study in optically complex waters of the temperate region. *Ecol. Indic.* 134, 108479. <https://doi.org/10.1016/j.ecolind.2021.108479>.
- Strokal, M., Kroeze, C., 2012. Nitrogen and phosphorus inputs to the Black Sea in 1970–2050. *Reg. Environ. Chang.* 13 (1), 179–192.
- Suikkanen, S., Pulina, S., Engström-Ost, J., Lehtiniemi, M., Lehtinen, S., Brutemark, A., 2013. Climate change and eutrophication induced shifts in northern summer plankton communities. *PLoS One* 8 (6), e66475. <https://doi.org/10.1371/journal.pone.0066475>.
- Suslin, V., Churilova, T., 2016. A regional algorithm for separating light absorption by chlorophyll-a and coloured detrital matter in the Black Sea, using 480–560 nm bands from ocean colour scanners. *Int. J. Remote Sens.* 37 (18), 4380–4400. <https://doi.org/10.1080/01431161.2016.1211350>.
- Sutula, M., Kudela, R., Hagy, J.D., Harding, L.W., Senn, D., Cloern, J.E., Bricker, S., Berg, G.M., Beck, M., 2017. Novel analyses of long-term data provide a scientific basis for chlorophyll-a thresholds in San Francisco Bay. *Estuar. Coast. Shelf Sci.* 197, 107–118. ISSN 0272-7714. <https://doi.org/10.1016/j.ecss.2017.07.009>.
- Sydeman, W., Bograd, S., 2009. Marine ecosystems, climate and phenology: introduction. *Mar. Ecol. Prog. Ser.* 393, 185–188. <https://doi.org/10.3354/meps08382>.
- Tamelerand, T., Spilling, K., Winder, M., 2017. Organic matter export to the seafloor in the Baltic Sea: drivers of change and future projections. *Ambio* 46 (8), 842–851. <https://doi.org/10.1007/s13280-017-0930-x>.
- Tilstone, G.H., Pardo, S., Dall'Olmo, G., Brewin, R.J.W., Nencioli, F., Dessailly, D., Kwiatkowska, E., Casal, T., Donlon, C., 2021. Performance of ocean colour chlorophyll algorithms for Sentinel-3 OLCI, MODIS-aqua and Suomi-VIIRS in open-ocean waters of the Atlantic. *Remote Sens. Environ.* 260, 112444 <https://doi.org/10.1016/j.rse.2021.112444>.
- Ueyama, R., Monger, B.C., 2005. Wind-induced modulation of seasonal phytoplankton blooms in the North Atlantic derived from satellite observations. *Limnol. Oceanogr.* 50 (6), 1820–1829. <https://doi.org/10.4319/lo.2005.50.6.1820>.
- Ummenhofer, C.C., Meehl, G.A., 2017. Extreme weather and climate events with ecological relevance: a review. *Philos. Trans. R. Soc. Lond. Ser. B Biol. Sci.* 372 (1723).
- United Nations (2021). The Second World Ocean Assessment. Volume I. United Nations publication, ISBN: 978-92-1-1-130422-0: 570 pp. <https://www.un.org/regularprocess/sites/www.un.org/regularprocess/files/201859-e-woa-ii-vol-i.pdf>.
- Van de Pol, M., Jenouvrier, S., Cornelissen, J.H.C., Visser, M.E., 2017. Behavioural, ecological and evolutionary responses to extreme climatic events: challenges and directions. *Philos. Trans. R. Soc. B* 372, 20160134. <https://doi.org/10.1098/rstb.2016.0134>.
- Vasconcelos, V., 2013. Emergent marine toxins in Europe: is there a new invasion? *J. Marine Sci. Res. Dev.* 3, e117 <https://doi.org/10.4172/2155-9910.1000e117>.
- Wei, G., Tang, D., Wang, S., 2008. Distribution of chlorophyll and harmful algal blooms (HABs): A review on space-based studies in the coastal environments of Chinese marginal seas. *Adv. Space Res.* 41 (1), 12–19. <https://doi.org/10.1016/j.asr.2007.01.037>.
- Winder, M., Cloern, J.E., 2010. The annual cycles of phytoplankton biomass. *Phil. Trans. R. Soc. B* 3653215–3226 <https://doi.org/10.1098/rstb.2010.0125>.
- World Health Organisation, 2003. Guidelines for safe recreational water environments. Volume 1: Coastal and Fresh Waters. ISBN 92 4 154580 1.
- Yunev, O.A., Carstensen, J., Stelmakh, L.V., Belokopytov, V.N., Suslin, V.V., 2021. Reconsideration of the phytoplankton seasonality in the open Black Sea. *Limnol. Oceanogr.* Lett. 6 (1), 51–59. <https://doi.org/10.1002/lo.21078>.
- Yunev, O., Carstensen, J., Stelmakh, L., Belokopytov, V., Suslin, V., 2022. Temporal changes of phytoplankton biomass in the western Black Sea shelf waters: evaluation by satellite data (1998–2018). *Estuar. Coast. Shelf Sci.* 271, 107865 <https://doi.org/10.1016/j.ecss.2022.107865>.
- Zhang, M., Zhang, Y., Qiao, F., Deng, J., Wang, G., 2017. Shifting trends in bimodal phytoplankton blooms in the North Pacific and North Atlantic oceans from space with the Holo-Hilbert spectral analysis. *IEEE J. Select. Top. Appl. Earth Observ. Remote Sens.* 10 (1), 57–64. <https://doi.org/10.1109/JSTARS.2016.2625813>.
- Zingone, A., Escalera, L., Aligizaki, K., Fernández-Tejedor, M., Ismael, A., Montresor, M., Mozetič, P., Taş, S., Totti, C., 2020. Toxic marine microalgae and noxious blooms in the Mediterranean Sea: A contribution to the Global HAB Status Report. *Harmful Algae*, 101843. ISSN 1568–9883. <https://doi.org/10.1016/j.hal.2020.101843>.